Electroweak structure of light nuclei and its implication for neutrino scattering

Electromagnetic interactions with nucleons and nuclei
EINN 2023 Paphos, Cyprus

1 November 2023
Saori Pastore

https://physics.wustl.edu/quantum-monte-carlo-group

Quantum Monte Carlo Group @ WashU
Lorenzo Andreoli (PD) Jason Bub (GS) Graham Chambers-Wall (GS) Garrett King (GS)
Anna McCoy (FRIB TA Fellow)
Maria Piarulli and Saori Pastore

Computational Resources awarded by the DOE ALCC, INCITE and SciDAC programs

Understand Nuclei to Understand the Cosmos

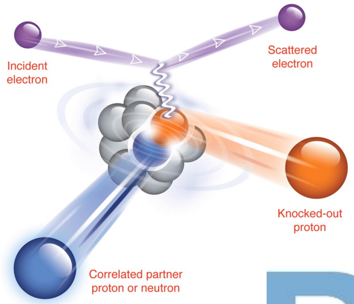

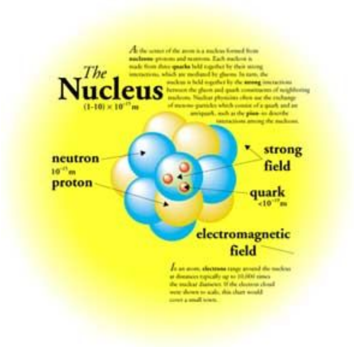

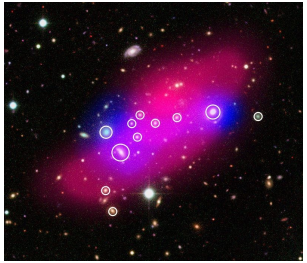

ESA, XMM-Newton, Gastaldello, CFHTL

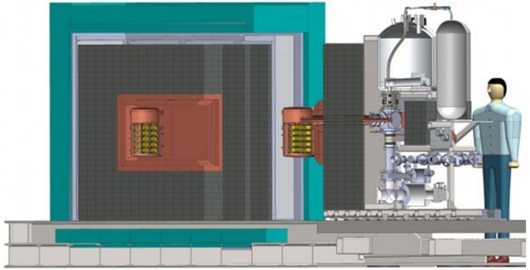

Ground States' Electroweak Moments, Form Factors, Radii

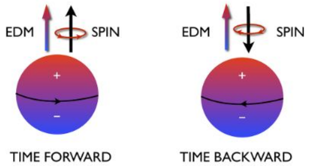

Neutrinoless Double Beta Decay, Muon-Capture

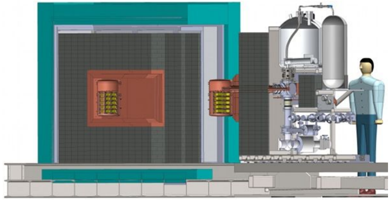

Accelerator Neutrino Experiments, Lepton-Nucleus XSecs

(ω,q)~0 MeV

ω~few MeVs
q~0 MeV

ω~few MeVs
q~10^2 MeV

ω~tens of MeVs

ω~10^2 MeV

FRIB

Electromagnetic Decay, Beta Decay, Double Beta Decay & inverse processes

JINA-CEE

Nuclear Rates for Astrophysics

DUNE

Jefferson Lab

Accelerator Neutrinos' Experiments

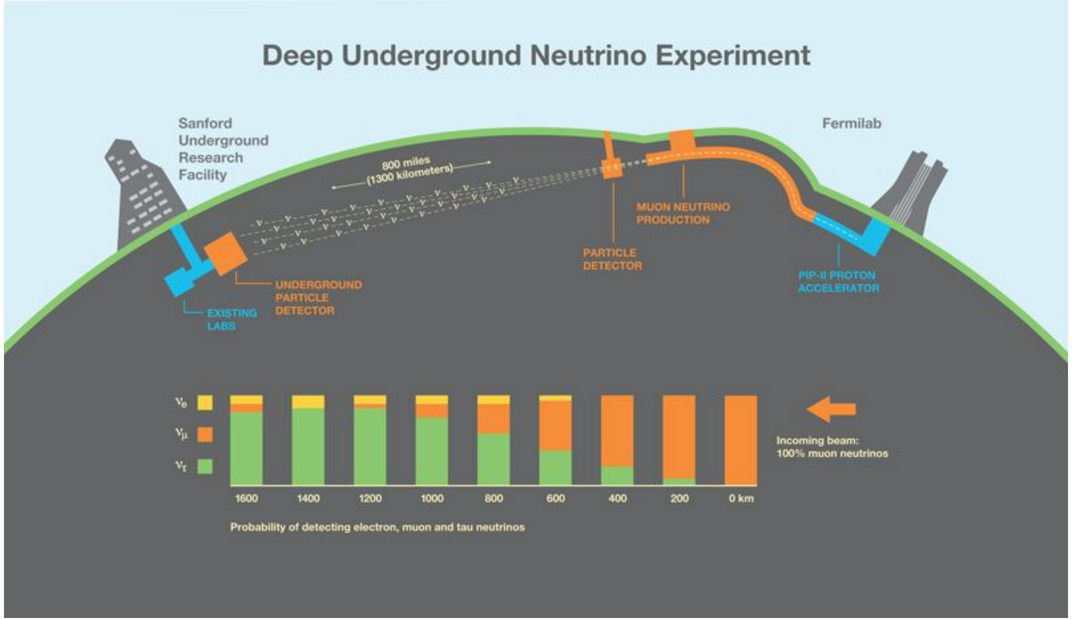

DUNE - Fermilab

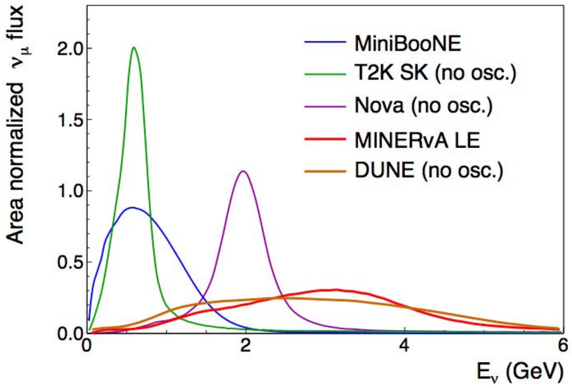

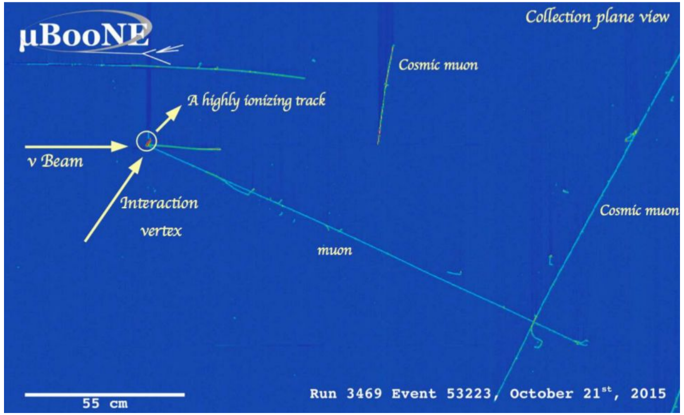

Nuclei for Neutrino Oscillations' Experiments

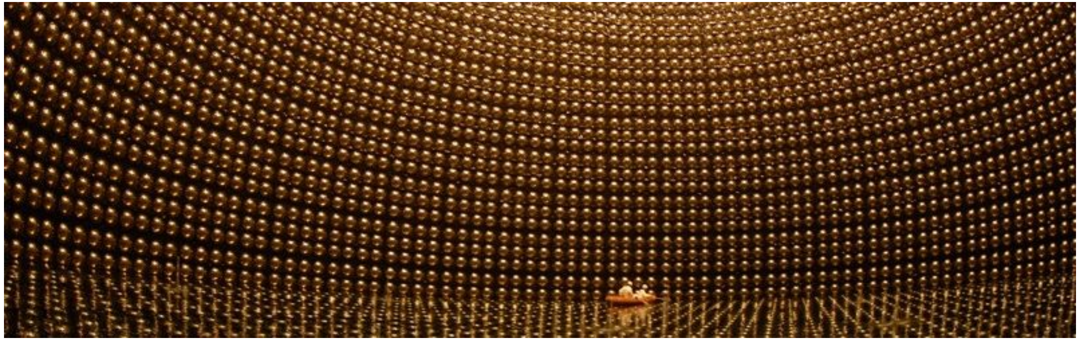

$$P(\nu_\mu \rightarrow \nu_e) = sin^2 2\theta sin^2\left(\frac{\Delta m_{21}^2 L}{2E_\nu}\right)$$

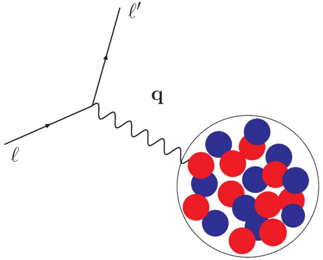

Nuclei are the active material in the detector. The energy of the incident neutrino is reconstructed from the observed final states using **neutrino event generators** that require **theoretical cross-sections**.

Neutrino-^{12}C cross section

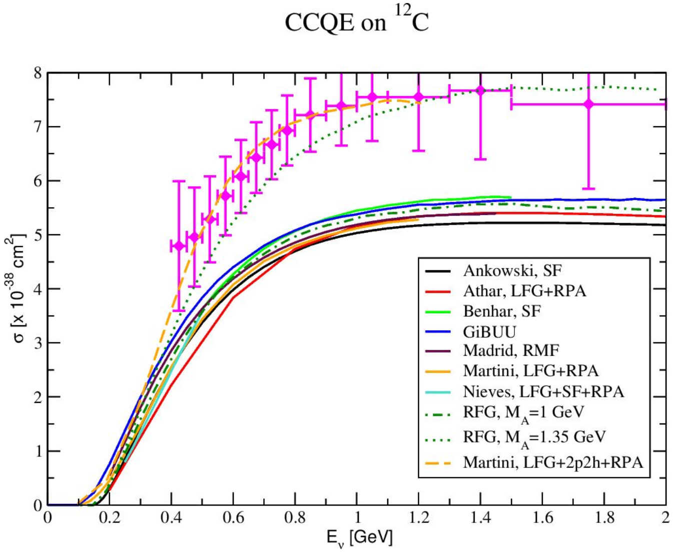

Alvarez-Ruso arXiv:1012.3871

Electron-Nucleus Scattering Cross Section

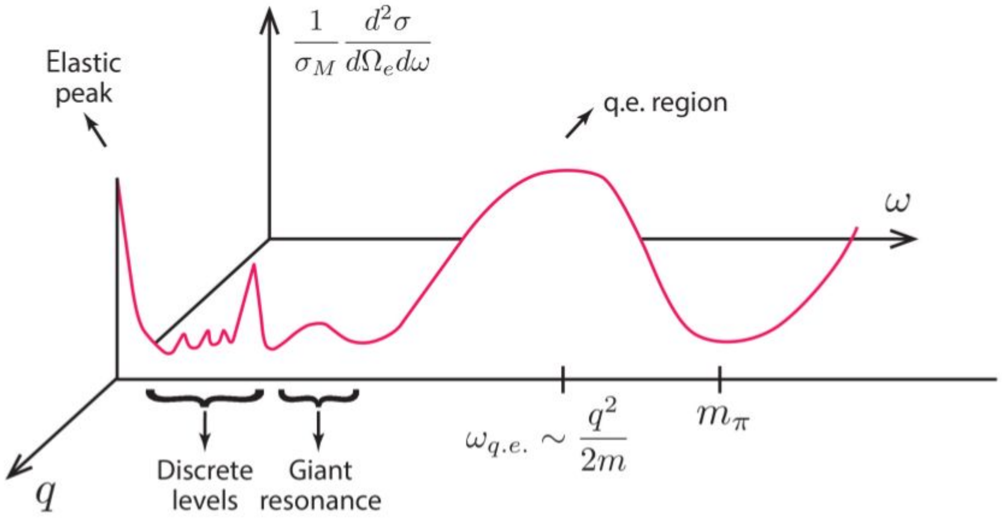

Energy and momentum transferred (ω,q)

Current and planned experimental programs rely on theoretical calculations at different kinematics

Strategy

Validate the Nuclear Model against available data for strong and electroweak observables

- Energy Spectra, Electromagnetic Form Factors, Electromagnetic Moments, ...
- Electromagnetic and Beta decay rates, ...
- Muon Capture Rates, ...
- Electron-Nucleus Scattering Cross Sections, ...

Use attained information to make (accurate) predictions for BSM searches and precision tests

- EDMs, Hadronic PV, ...
- BSM searches with beta decay, ...
- Neutrinoless double beta decay, ...
- Neutrino-Nucleus Scattering Cross Sections, ...
- ...

From Quarks to Nuclei

- Nuclei are complex systems made of interacting protons and neutrons, which in turns are composite objects made of interacting constituent quarks.
- All fundamental forces are at play in nuclei.
- **EFTs** low-energy approximations of QCD whose d.o.f. are bound states of QCD (e.g., protons, neutrons, pions, …)
- **EFTs** are used to construct many-nucleon interactions and currents

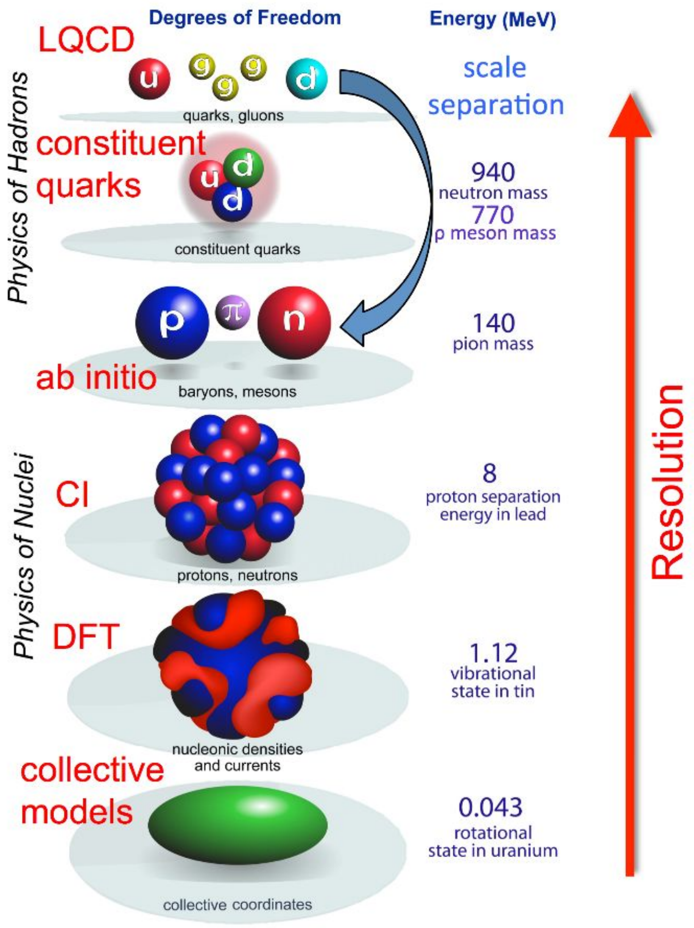

Microscopic (or *ab initio*) Description of Nuclei

Comprehensive theory that describes quantitatively and predictably nuclear structure and reactions

Requirements:

- Accurate understanding of the interactions/correlations between nucleons in **paris**, **triplets**, ... (**two- and three-nucleon forces**)
- Accurate understanding of the electroweak interactions of external probes (electrons, neutrinos, photons) with nucleons, correlated nucleon-pairs, … (**one- and two-body electroweak currents**)
- **Computational methods** to solve the many-body nuclear problem of strongly interacting particles

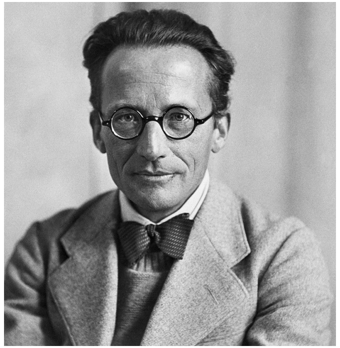

Erwin Schrödinger

$$H\Psi = E\Psi$$

Many-body Nuclear Problem

Nuclear Many-body Hamiltonian

$$H = T + V = \sum_{i=1}^{A} t_i + \sum_{i<j} v_{ij} + \sum_{i<j<k} V_{ijk} + \ldots$$

$$\Psi(\mathbf{r}_1, \mathbf{r}_2, \ldots, \mathbf{r}_A, s_1, s_2, \ldots, s_A, t_1, t_2, \ldots, t_A)$$

Ψ are spin-isospin vectors in 3A dimensions with $2^A \times \frac{A!}{Z!(A-Z)!}$ components

Develop Computational Methods to solve (numerically) exactly or within approximations that are under control the many-body nuclear problem

http://exascaleage.org/np/

^{4}He : 96
^{6}Li : 1280
^{8}Li : 14336
^{12}C : 540572

Current Status

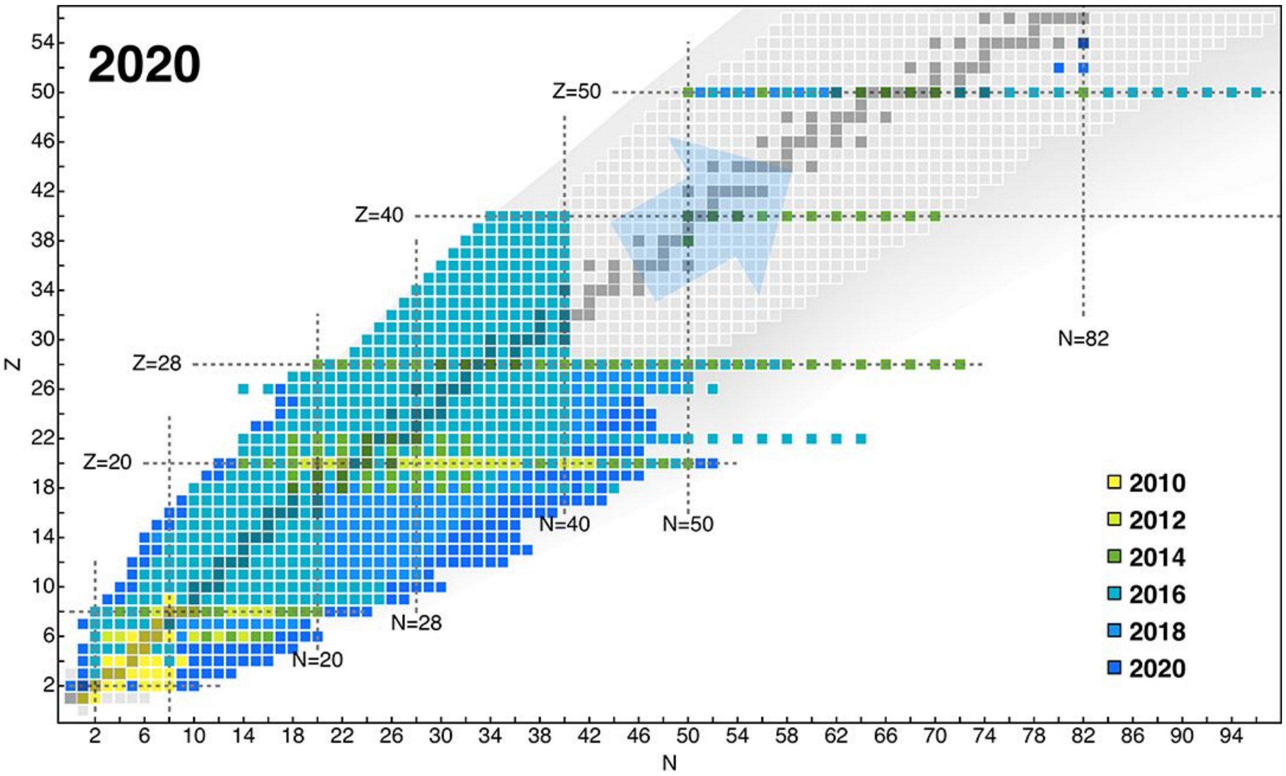

H. Hergert
Front. Phys.
07 October 2020

Many-body Nuclear Interactions

Many-body Nuclear Hamiltonian

$$H = T + V = \sum_{i=1}^{A} t_i + \sum_{i<j} v_{ij} + \sum_{i<j<k} V_{ijk} + \ldots$$

v_{ij} and V_{ijk} are two- and three-nucleon operators based on experimental data fitting; fitted parameters subsume underlying QCD dynamics

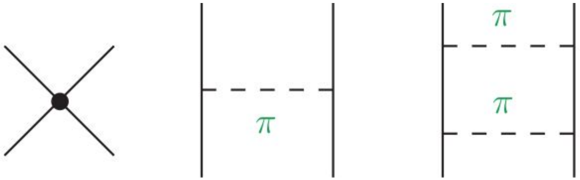

Contact term: short-range
Two-pion range: intermediate-range $r \propto (2\,m_\pi)^{-1}$
One-pion range: long-range $r \propto m_\pi^{-1}$

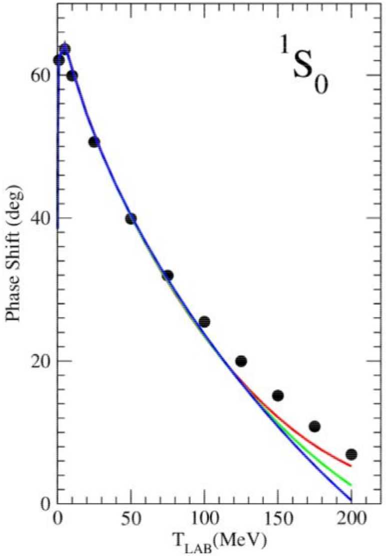

SP et al. PRC80(2009)034004

Hideki Yukawa

AV18+UIX; AV18+IL7
Wiringa, Schiavilla, Pieper *et al*.

chiral πNΔ
N3LO+N2LO Piarulli *et al*. **Norfolk Models**

Energies

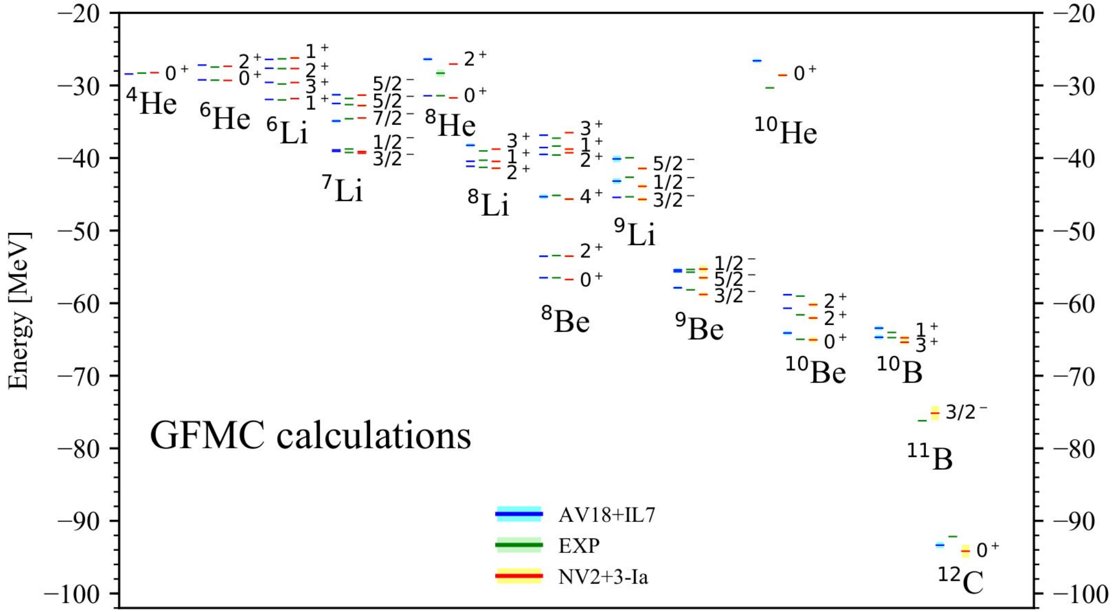

Piarulli *et al.* PRL120(2018)052503

Many-body Nuclear Electroweak Currents

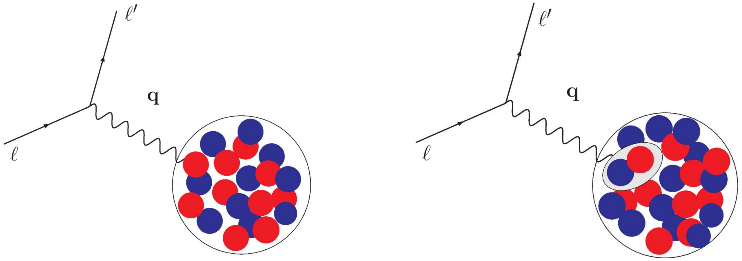

one-body

two-body

- Two-body currents are a manifestation of two-nucleon correlations
- Electromagnetic two-body currents are required to satisfy current conservation

$$\mathbf{q}\cdot\mathbf{j} = [\,H,\,\rho\,] = [t_i + v_{ij} + V_{ijk},\,\rho\,]$$

Nuclear Charge Operator

$$\rho = \sum_{i=1}^{A} \rho_i + \sum_{i<j} \rho_{ij} + \ldots$$

Nuclear (Vector) Current Operator

$$\mathbf{j} = \sum_{i=1}^{A} \mathbf{j}_i + \sum_{i<j} \mathbf{j}_{ij} + \ldots$$

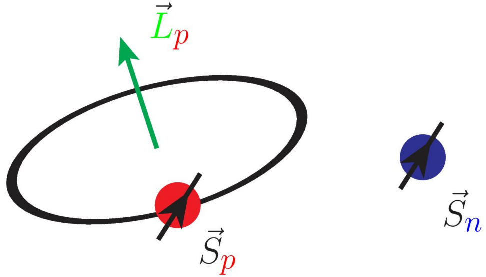

Magnetic Moment: Single Particle Picture

Many-body Currents

- **Meson Exchange Currents** (MEC)

Constrain the MEC current operators by imposing that the current conservation relation is satisfied with the given two-body potential

- **Chiral Effective Field Theory Currents**

Are constructed consistently with the two-body chiral potential; Unknown parameters, or Low Energy Constants (**LECs**), need to be **determined by either fits to experimental data or by Lattice QCD calculations**

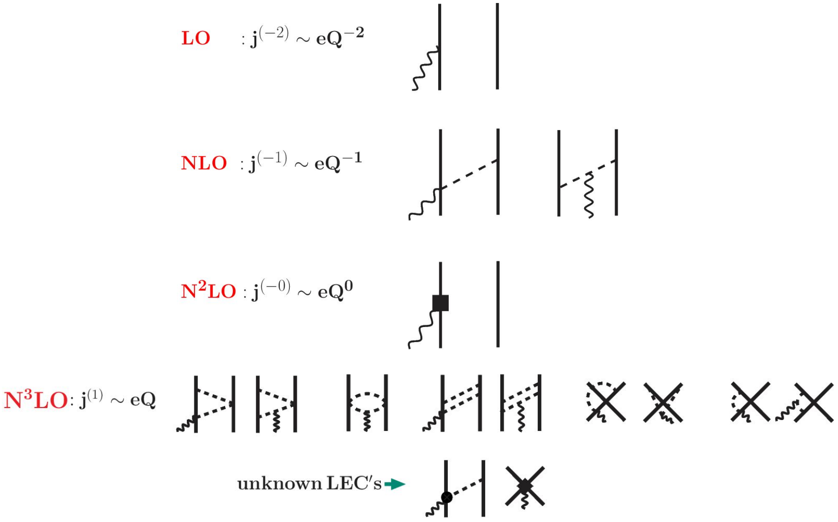

Electromagnetic Current Operator

SP *et al.* PRC78(2008)064002, PRC80(2009)034004, PRC84(2011)024001, PRC87(2013)014006
Park *et al.* NPA596(1996)515, Phillips (2005)
Kölling *et al.* PRC80(2009)045502 & PRC84(2011)054008

LCQD inputs for neutrino-nucleus scattering

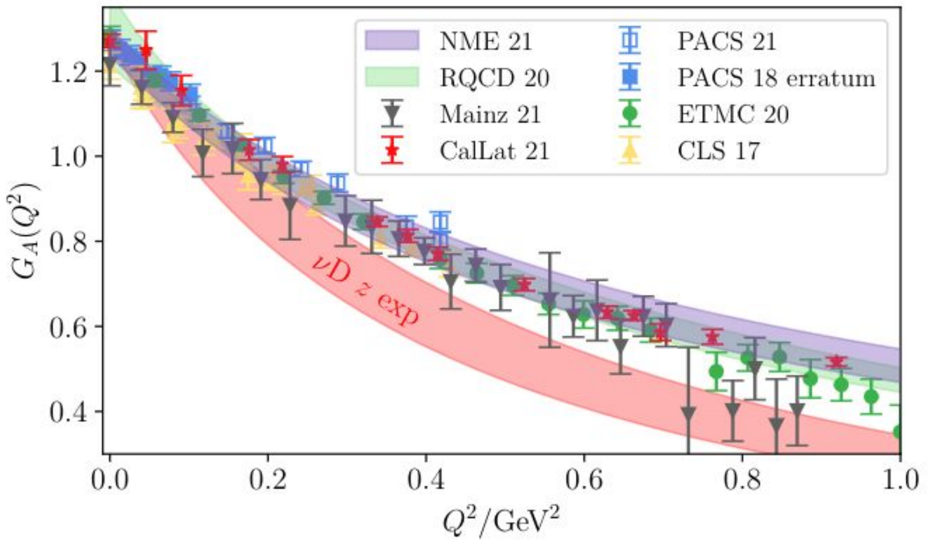

Snowmass WP: Theoretical tools for neutrino scattering: interplay between lattice QCD, EFTs, nuclear physics, phenomenology, and neutrino event generators; arXiv:2203.09030

Meyer, Walker-Loud, Wilkinson (2022)

Building blocks of ab initio nuclear approaches:

Nucleonic form factors
Transition form factors
Pion production amplitudes
Two-nucleon couplings (strong and EW)
…

Taken from data where available, or from theory

See talks by Bacchio, Koutsou, Tomalak, …

Magnetic Moments of Light Nuclei

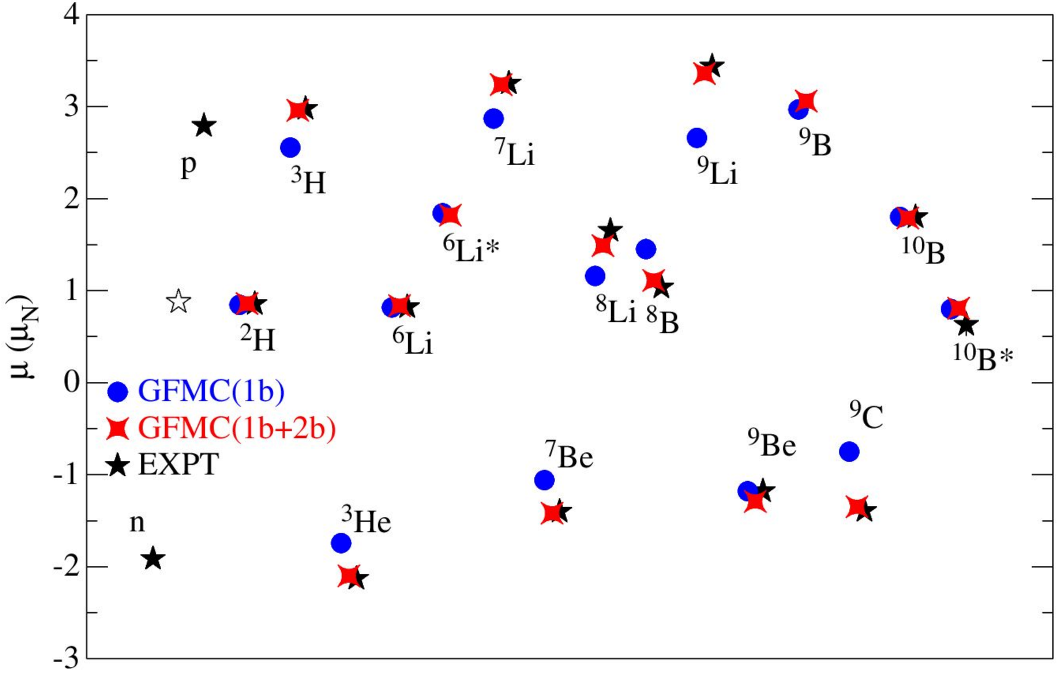

SP *et al*. PRC87(2013)035503

Single particle picture

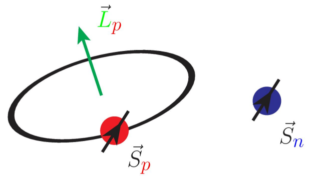

$$\mu_N(1\text{b}) = \sum_i [(L_i + g_p S_i)(1+\tau_{i,z})/2 + g_n S_i (1-\tau_{i,z})/2]$$

Small two-body current effects

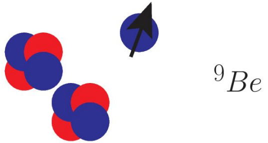

Large two-body current effects

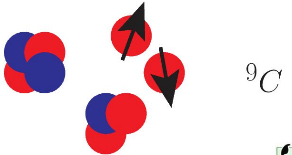

Electromagnetic form factors from chiEFT

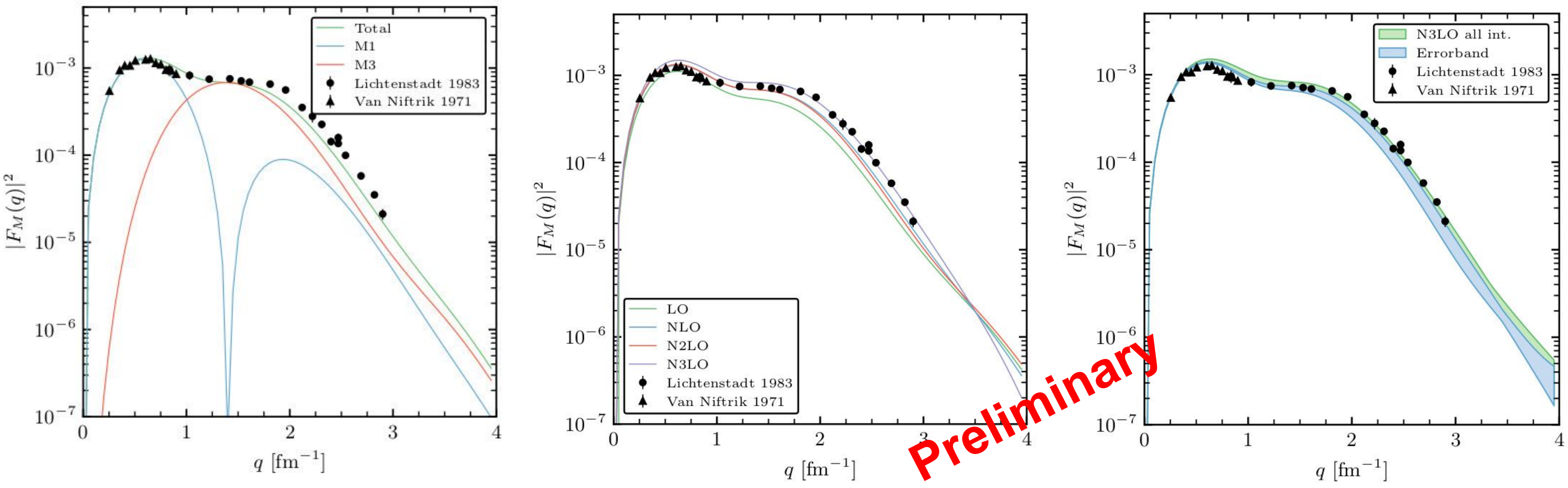

^{7}Li magnetic form factor - A. Gnech, G. Chambers-Wall, G. King *et al.* (in preparation)

Electromagnetic Observables

Magnetic moments

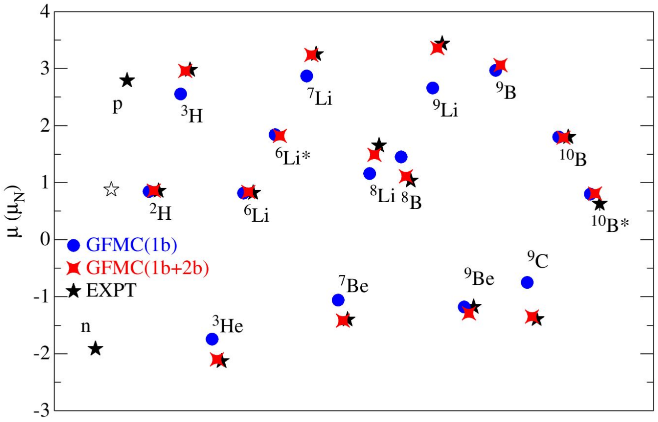

SP *et al*. PRC87(2013)035503, PRC101(2020)044612

EM decay

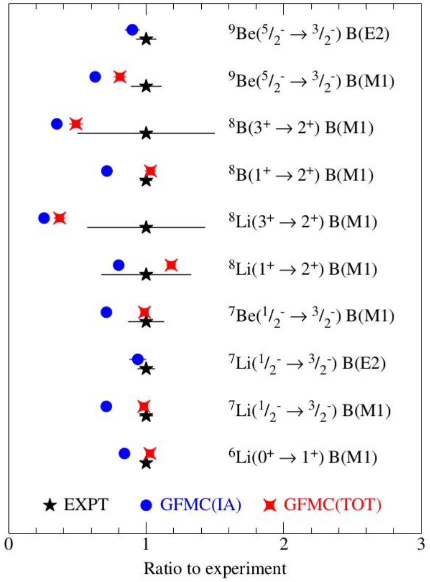

e-^{4}He particle scattering

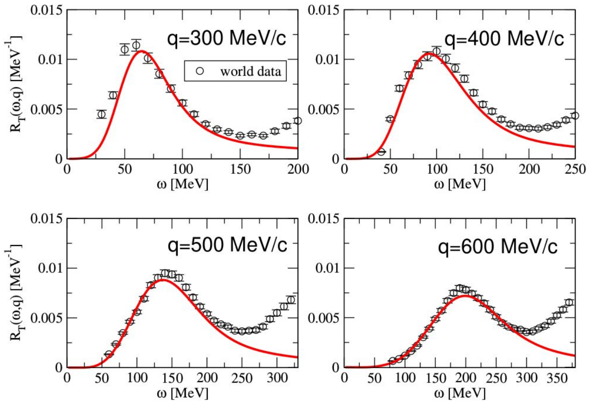

Axial currents with Δ at tree-level

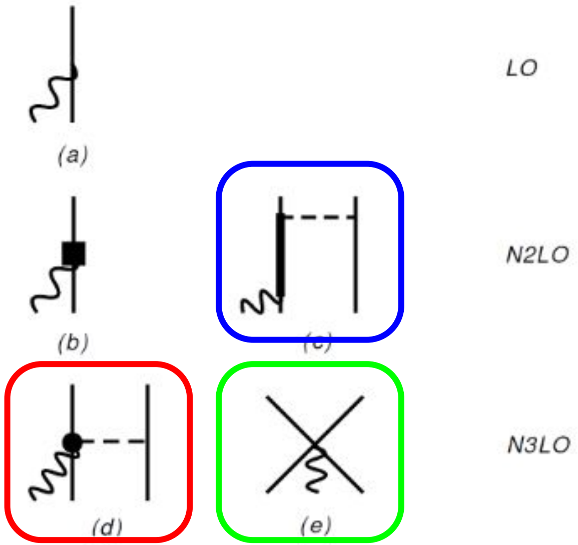

Two body currents of one pion range (red and blue) with c_3 c_4 from Krebs *et al.* Eur.Phys.J.(2007)A32

Contact current involves the LEC c_D

Beta decay

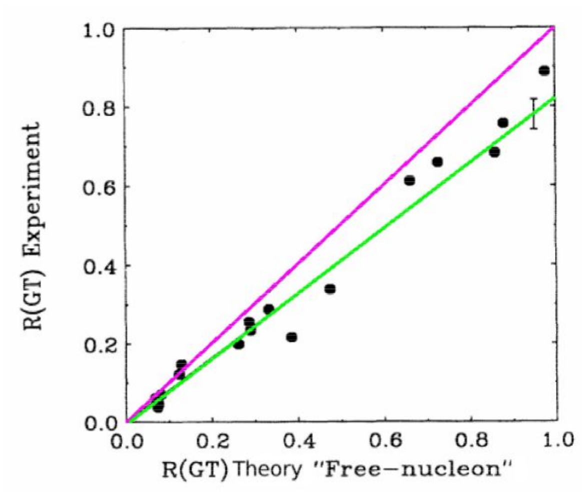

Chou et al. PRC47(1993)163

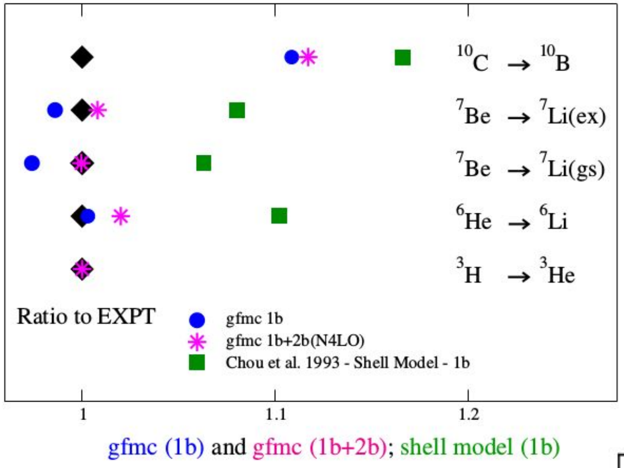

SP *et al*. PRC97(2018)022501

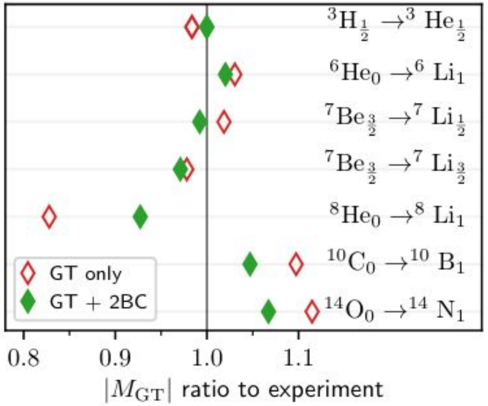

P. Gysbers *Nature Phys.* 15 (2019)

Beta decay spectrum

^{6}He Beta decay spectrum for BSM searches with NCSL, He6-CRES, LPC-Caen

Standard Model spectrum for ^{6}He

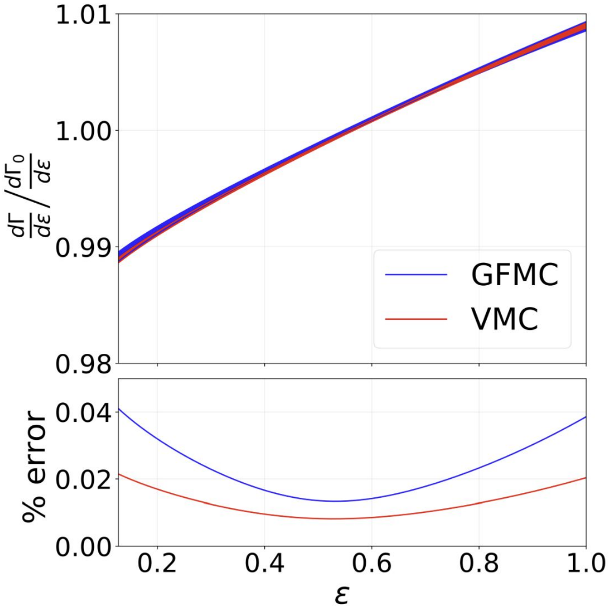

$$\varepsilon = \frac{E_e}{\omega}$$

$$\frac{d\Gamma}{d\varepsilon} = \frac{d\Gamma_0}{d\varepsilon} \times (1 + \text{corrections})$$

Garrett King et al. PRC (2023)

Partial muon capture rates: VMC calculations

$\Gamma_{VMC}(\text{avg.}) = 1495\ s^{-1} \pm 19\ s^{-1}$

$\Gamma_{expt} = 1496.0\ s^{-1} \pm 4.0\ s^{-1}$

Ackerbauer *et al.* PLB417, 224(1998)

Momentum transfer **q~ 100 MeV**

Two-body correction is ~8% of total rate on average for A=3

Garrett King *et al.* PRC2022

Review by Measday [Physics Reports 354 (2001) 243–409]

$^3He(1/2^+;1/2) \rightarrow {}^3H(1/2^+;1/2)$

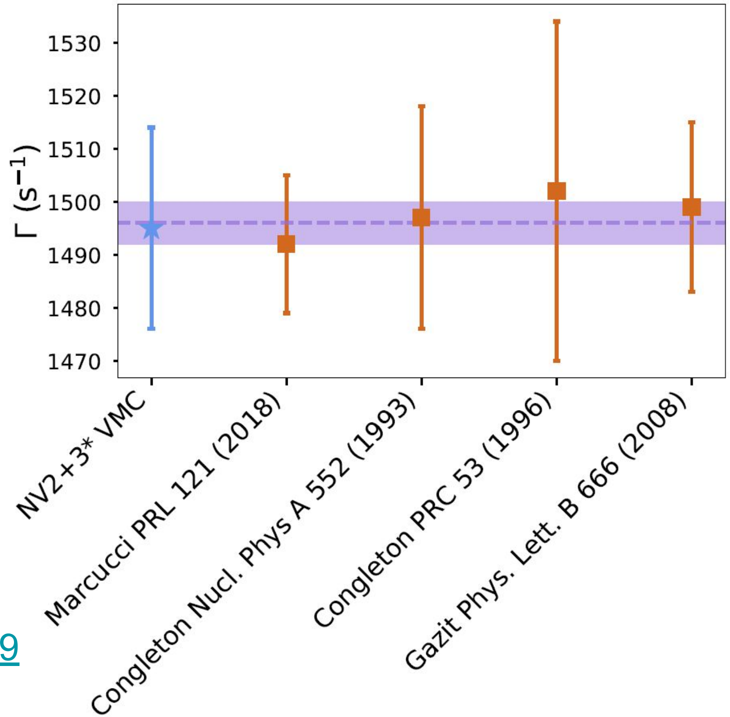

Neutrino cross section anatomy

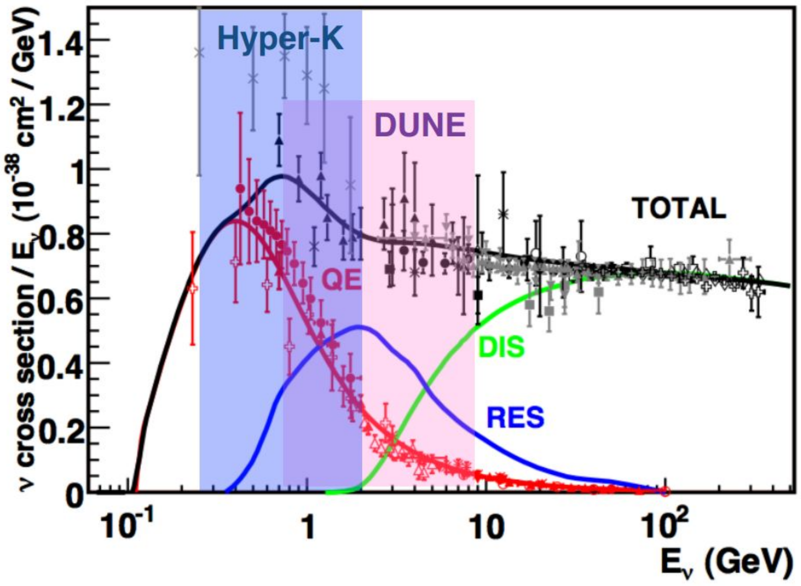

Formaggio & Zeller

Quasi-elastic: dominated by single-nucleon knockout

Resonance: excitation to nucleonic resonant states which decay into mesons

Deep-inelastic scattering: where the neutrino resolves the nucleonic quark content

Each of these regimes requires knowledge of both the **nuclear ground state** and the **electroweak coupling** and **propagation of the struck nucleons, hadrons, or partons**

A challenge for achieving precise neutrino-nucleus cross-section is **reliably bridging the transition regions which use different degrees of freedom**

Lepton-Nucleus scattering: Inclusive Processes

Electromagnetic Nuclear Response Functions

$$R_\alpha(q,\omega) = \sum_f \delta\left(\omega + E_0 - E_f\right) |\langle f|O_\alpha(\mathbf{q})|0\rangle|^2$$

Longitudinal response induced by the charge operator $O_L = \rho$
Transverse response induced by the current operator $O_T = \boldsymbol{j}$
5 Responses in neutrino-nucleus scattering

$$\frac{d^2\sigma}{d\omega d\Omega} = \sigma_M \left[v_L R_L(\mathbf{q},\omega) + v_T R_T(\mathbf{q},\omega)\right]$$

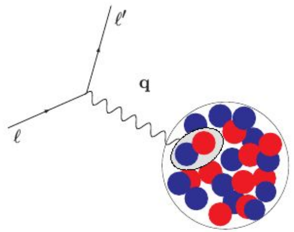

For a recent review on QMC, SF methods see
Rocco *Front. In Phys.*8 (2020)116

Inclusive Cross Sections with Integral Transforms

Exploit integral properties of the response functions and closure to avoid explicit calculation of the final states (Lorentz Integral Transform **LIT**, **Euclidean**, …)

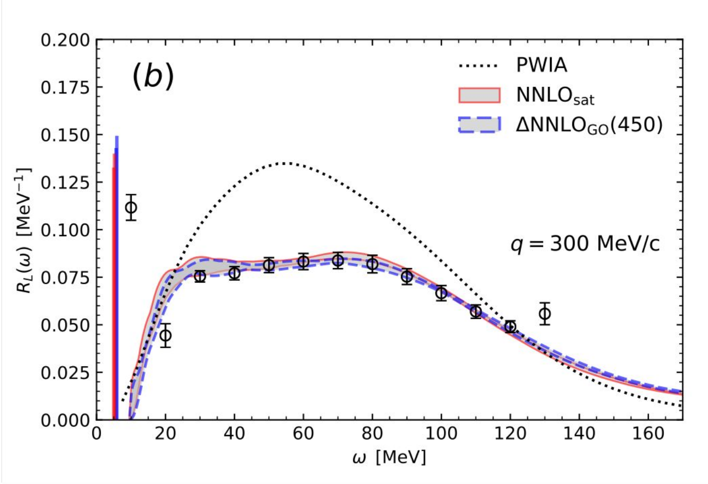

Sobczyk et al, PRL127 (2021)

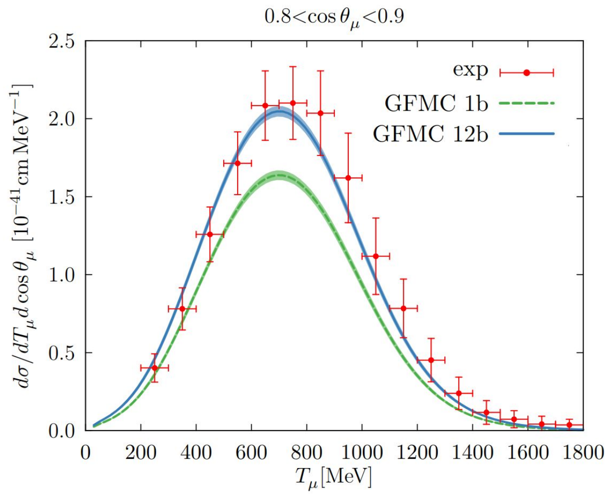

Lovato et al. PRX10 (2020)

Lepton-Nucleus scattering: Data

Transverse Sum Rule

$$S_T(q) \propto \langle 0|\mathbf{j}^\dagger\ \mathbf{j}|0\rangle \propto \langle 0|\mathbf{j}_{1b}{}^\dagger\ \mathbf{j}_{1b}|0\rangle + \langle 0|\mathbf{j}_{1b}{}^\dagger\ \mathbf{j}_{2b}|0\rangle + \dots$$

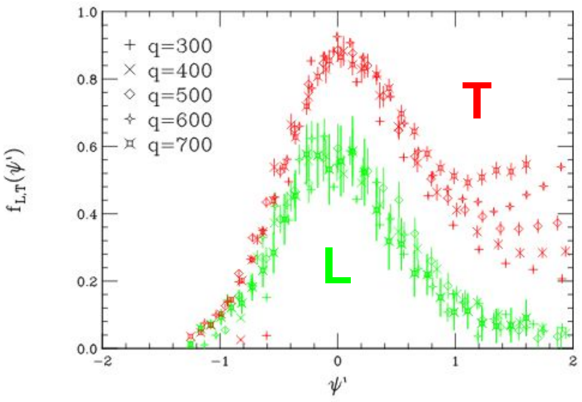

^{4}He Electromagnetic Data
Carlson *et al.* PRC65(2002)024002

Observed transverse enhancement explained by the combined effect of two-body correlations and currents in the interference term

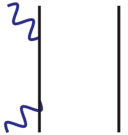

$\langle \mathbf{j}_{1b}^\dagger\ \ \mathbf{j}_{1b}\rangle\ > 0$

Leading one-body term

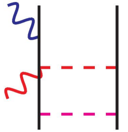

$\langle \mathbf{j}_{1b}^\dagger\ \mathbf{j}_{2b}\ v_\pi\rangle \propto \langle v_\pi^2\rangle\ > 0$

Interference term

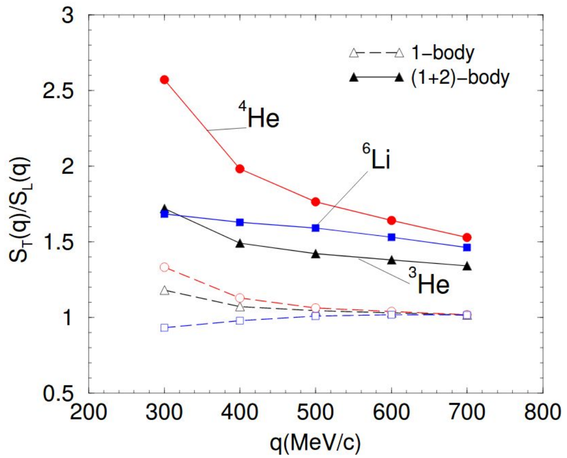

Transverse/Longitudinal Sum Rule
Carlson *et al.* PRC65(2002)024002

Beyond Inclusive: Short-Time-Approximation

Short-Time-Approximation Goals:

- Describe electroweak scattering from A > 12 without losing two-body physics
- Account for exclusive processes
- Incorporate relativistic effects

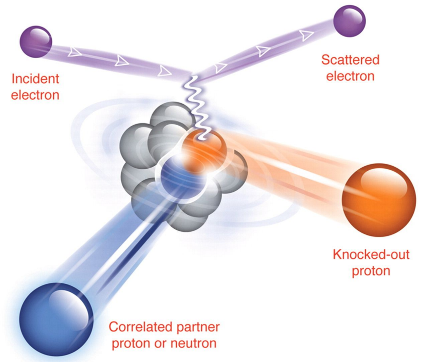

Subedi et al. Science320(2008)1475

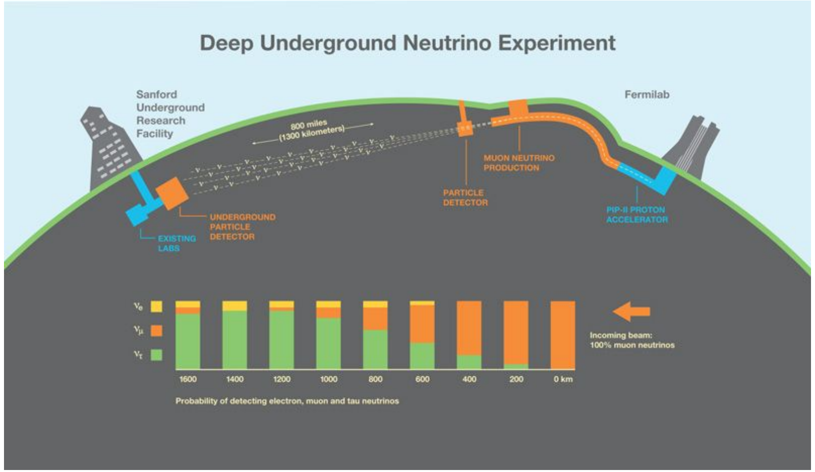

Stanford Lab article

e4u collaboration

Short-Time-Approximation

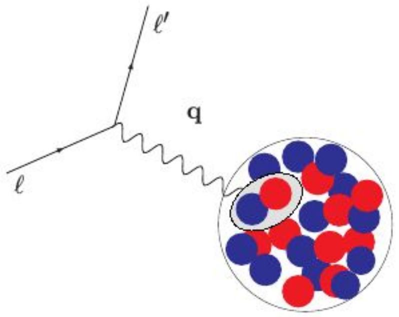

Short-Time-Approximation:

- Based on Factorization (also SF by Noemi Rocco)
- Retains two-body physics
- Correctly accounts for interference

$$R(q,\omega) = \int_{-\infty}^{\infty} \frac{dt}{2\pi} e^{i(\omega+E_0)t} \langle 0|O^\dagger e^{-iHt} O|0\rangle$$

$$O_i^\dagger e^{-iHt} O_i + O_i^\dagger e^{-iHt} O_j + O_i^\dagger e^{-iHt} O_{ij} + O_{ij}^\dagger e^{-iHt} O_{ij}$$

$$H \sim \sum_i t_i + \sum_{i<j} v_{ij}$$

STA: regime of validity

The typical (conservative estimate) energy (time) scale in a nucleus with A correlated nucleons in pairs is

$\varepsilon_{pair} \sim 20$ MeV   ($t \sim 1/\varepsilon_{pair}$)

This sets a natural expansion parameter in the QE region characterized by ω_{QE}

$\varepsilon_{pair} / \omega_{QE}$

The STA neglects terms of order $\mathcal{O}((\varepsilon_{pair} / \omega_{QE})^2)$

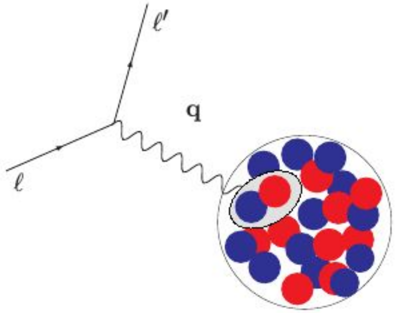

Short-Time-Approximation

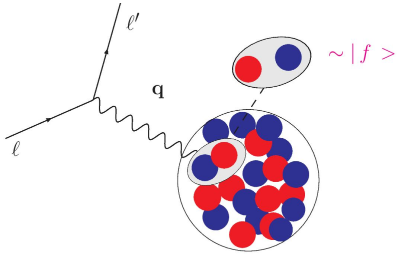

Short-Time-Approximation:

- Based on Factorization
- **Retains two-body physics**
- Response functions are given by the **scattering from pairs of fully interacting nucleons** that propagate into a correlated pair of nucleons
- Allows to retain both two-body correlations and currents at the vertex
- Provides "more" exclusive information in terms of nucleon-pair kinematics via the Response Densities

Response Functions ∝ Cross Sections

$$R_\alpha(q,\omega) = \sum_f \delta\left(\omega + E_0 - E_f\right) |\langle f|O_\alpha(\mathbf{q})|0\rangle|^2$$

Response ***Densities***

$$R(q,\omega) \sim \int \delta\left(\omega + E_0 - E_f\right)\, dP'\, dp' \mathcal{D}(p', P'; q)$$

P' and *p'* are the CM and relative momenta of the struck nucleon pair

Transverse Response Density: e-^{4}He scattering

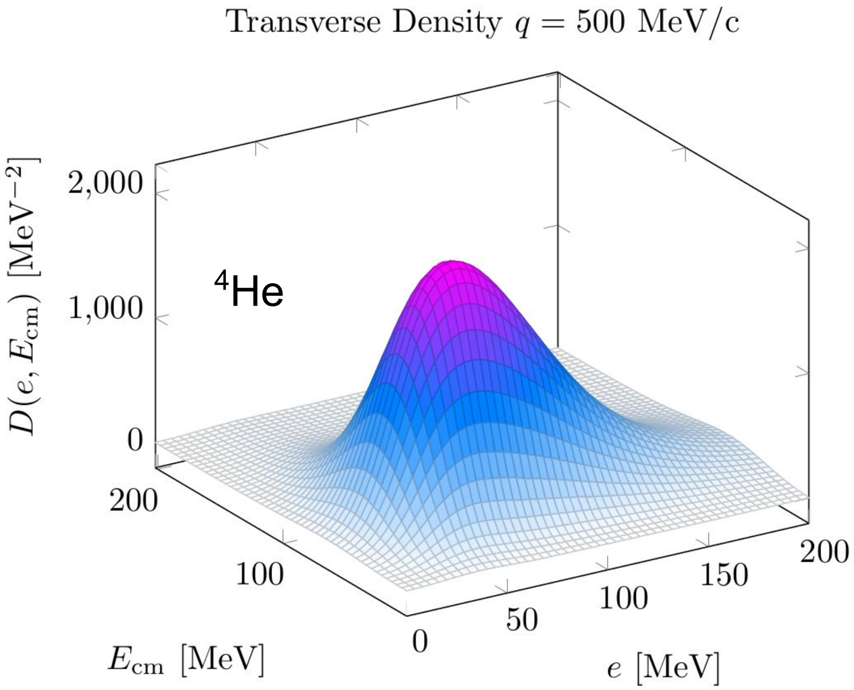

SP *et al.* PRC101(2020)044612

e-^{4}He scattering in the back-to-back kinematic

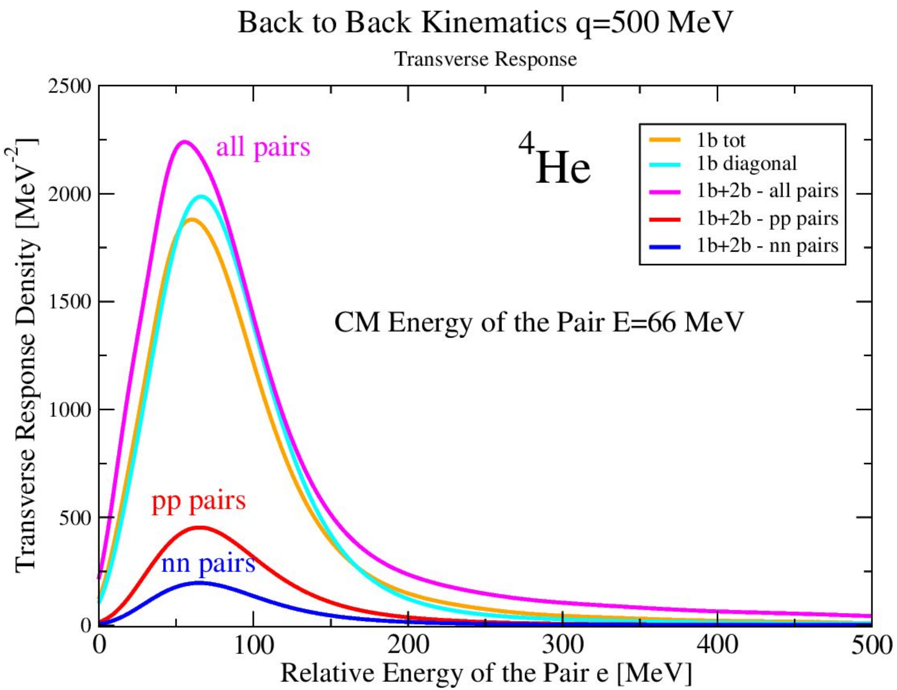

SP *et al.* PRC101(2020)044612

- pp pairs
- nn pairs
- all pairs 1body
- all pairs tot

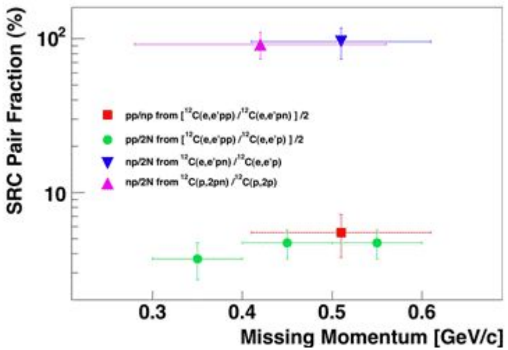

Subedi et al. Science320(2008)1475

GENIE validation using e-scattering

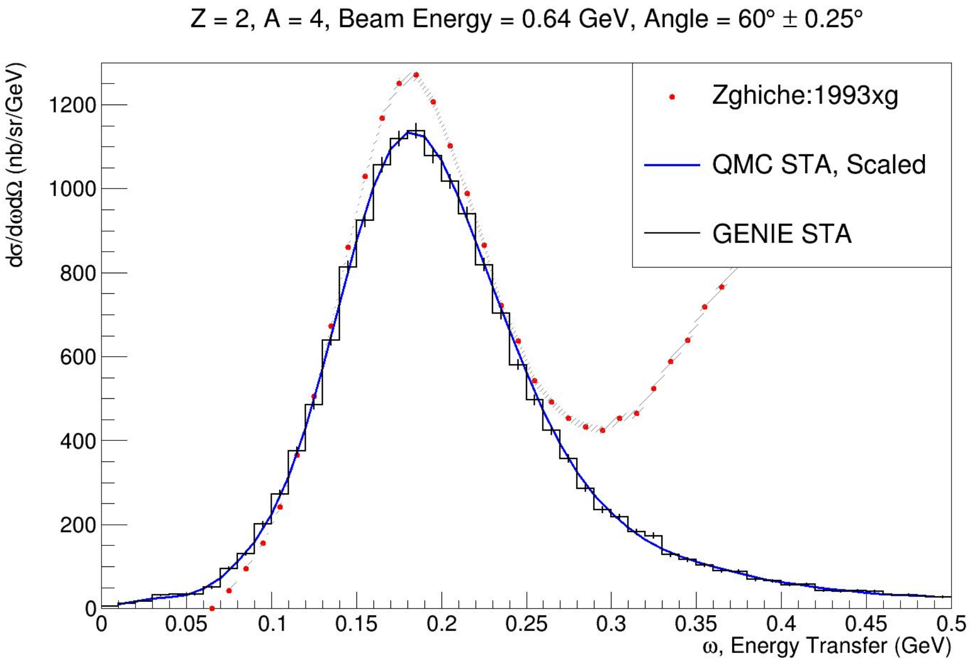

Barrow, Gardiner, SP et al. PRD 103 (2021) 5, 052001

- STA responses used to build the cross sections
- Cross sections are used to generate events in GENIE (a Monte Carlo neutrino event generator)
- Here, we use electromagnetic processes (for which data are available) to validate the generator

$$\frac{d^2\sigma}{d\omega d\Omega} = \sigma_M \left[v_L R_L(\mathbf{q},\omega) + v_T R_T(\mathbf{q},\omega) \right]$$

GFMC SF STA: Benchmark & error estimate

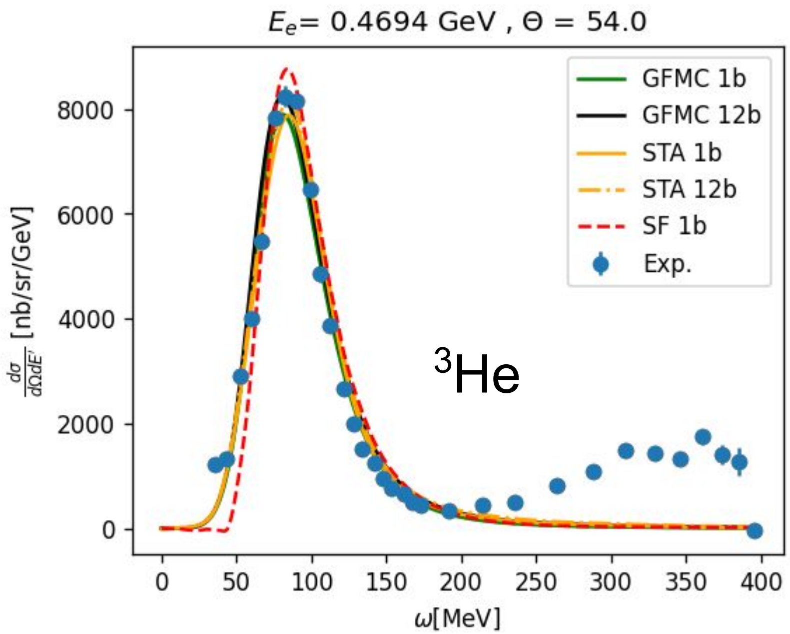

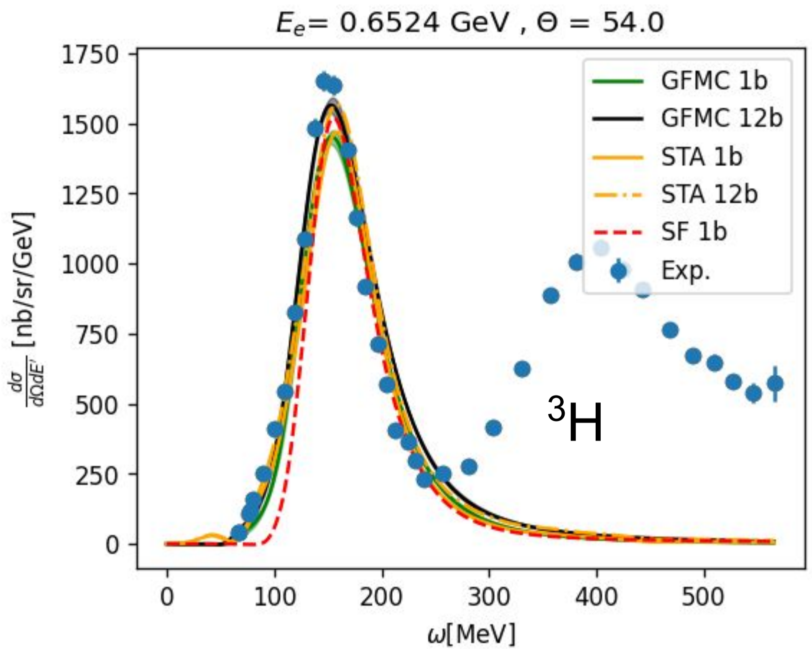

Lorenzo Andreoli, *et al.* PRC 2021

Importance of relativistic corrections

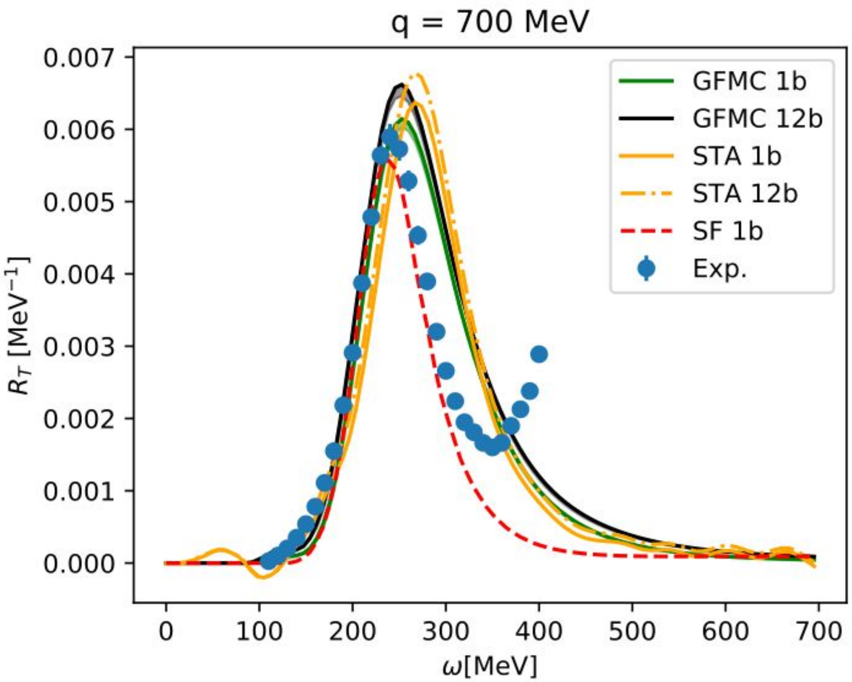

Lorenzo Andreoli, *et al.* PRC 2021

(Available) Mainz kinematics

E_e = 855 MeV θ_e = 70

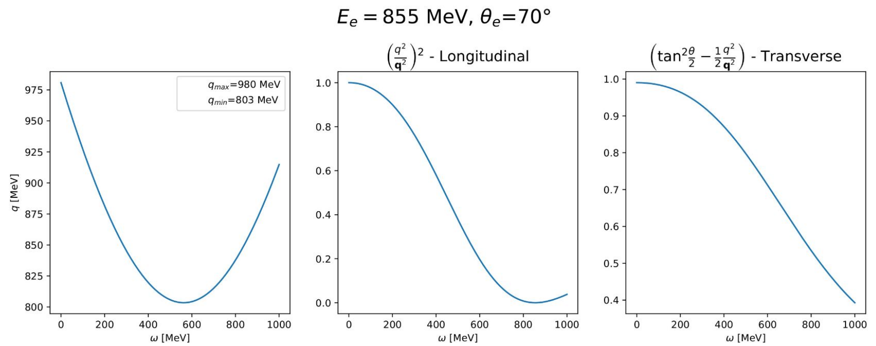

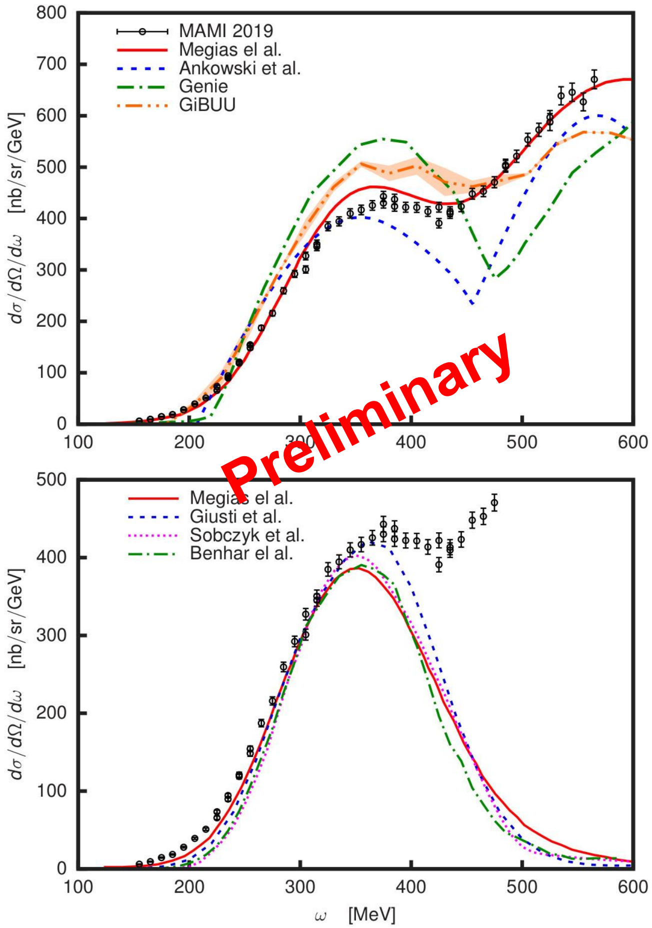

Relativistic corrections

So far we used non relativistic reduction of the single nucleon covarian current (low-momentum expansion both p and p')

With Ronen Weiss

Relativistic corrections obtained expanding the covariant one-nucleon current for high values of momentum transfer **q**

$$j^\mu = e\bar{u}(\boldsymbol{p}'s')\left(e_N\gamma^\mu + \frac{i\kappa_N}{2m_N}\sigma^{\mu\nu}q_\nu\right)u(\boldsymbol{p}s)$$

$$\boldsymbol{p}' = \boldsymbol{p} + \boldsymbol{q}$$

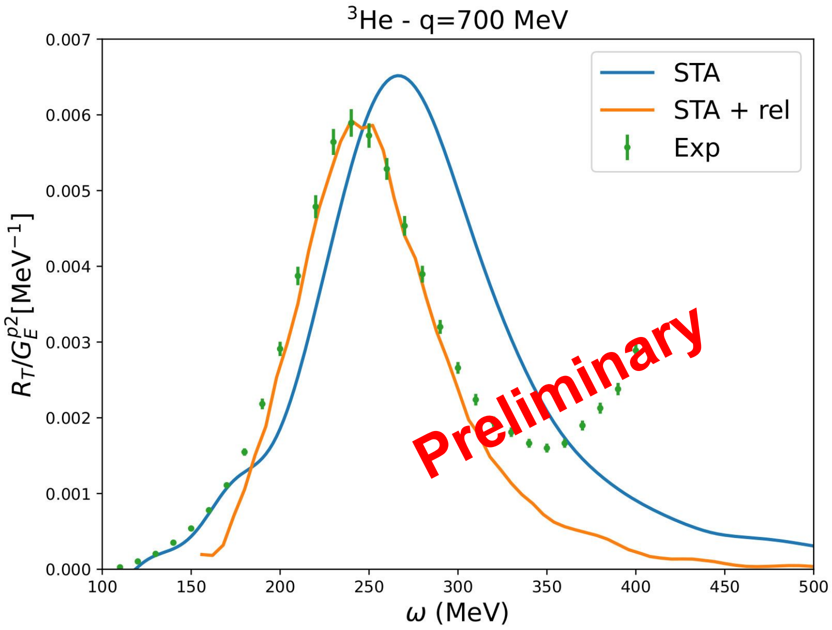

R. Weiss & L. Andreoli *et al.* (in preparation)

Towards A=12

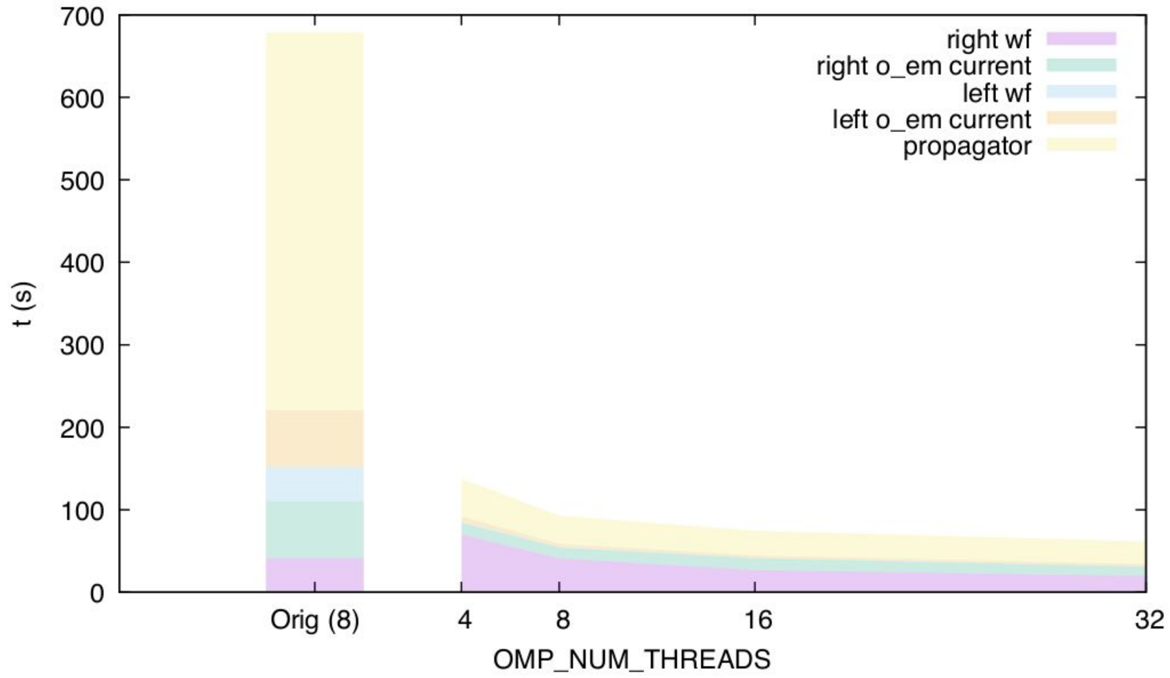

Lorenzo Andreoli
et al. in preparation

$$R_\alpha(q,\omega) = \int_{-\infty}^{\infty} \frac{dt}{2\pi} e^{i(\omega+E_i)t} \langle \Psi_i | O_\alpha^\dagger(\mathbf{q}) e^{-iHt} O_\alpha(\mathbf{q}) | \Psi_i \rangle$$

^{12}C Response Densities

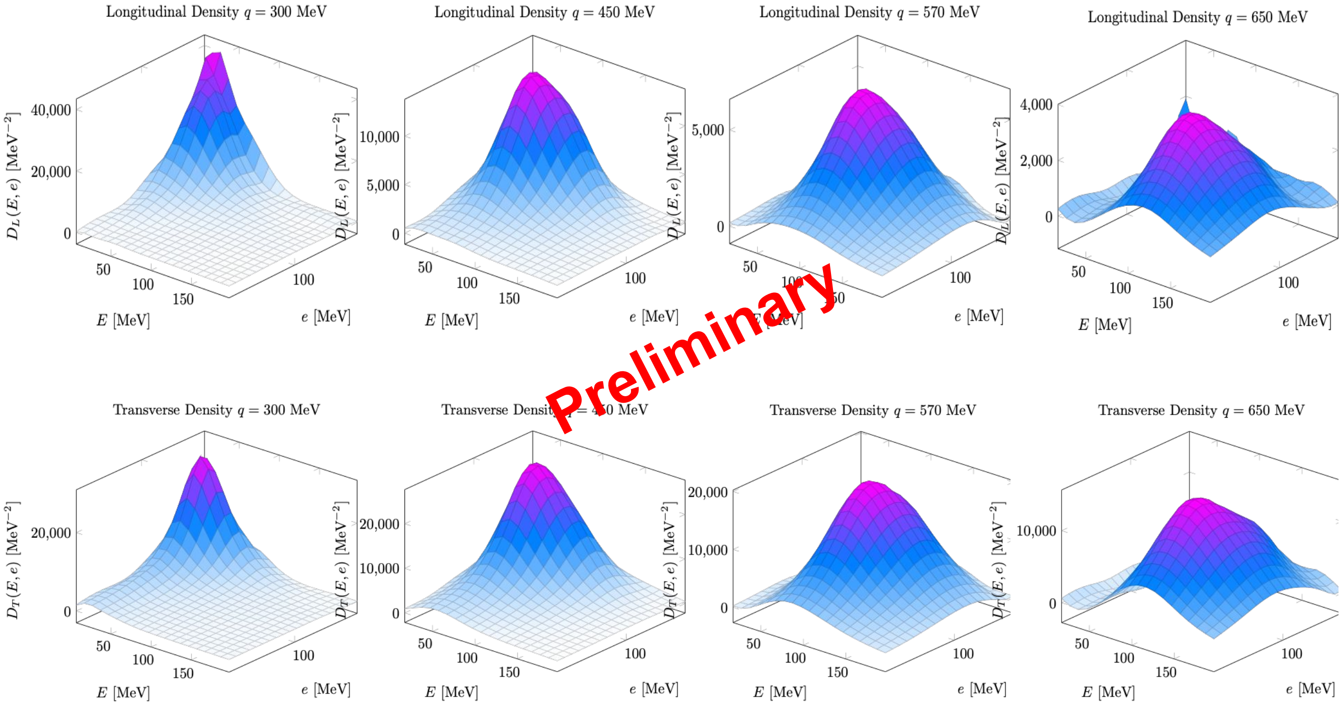

Lorenzo Andreoli *et al.* in preparation

^{12}C cross sections: interpolation scheme

We have coarse grid in q for ^{12}C. We use an interpolation scheme tested on He4.

$$I_{L/T}(\omega;\mathbf{q}) = \frac{\int_0^{\omega} R_{L/T}(\omega';\mathbf{q})d\omega'}{\int_0^{\infty} R_{L/T}(\omega';\mathbf{q})d\omega'}$$

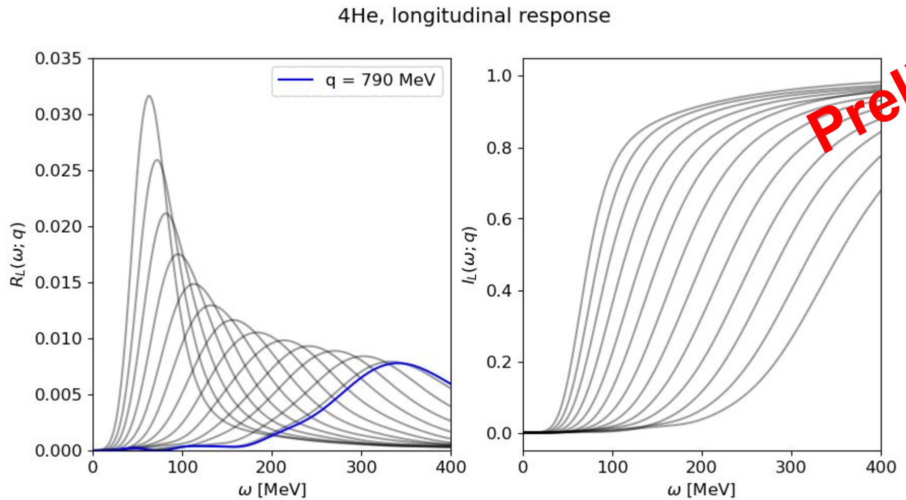

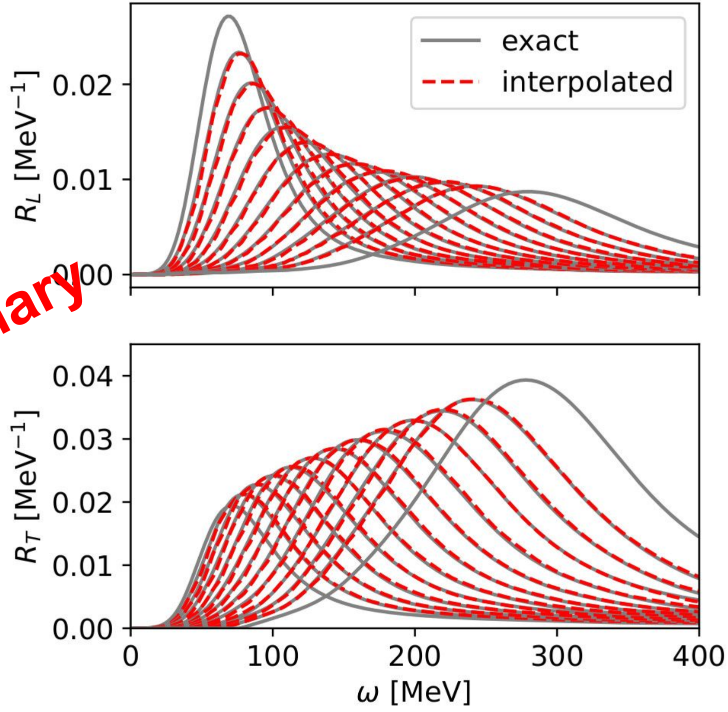

Preliminary

Lorenzo Andreoli *et al.* in preparation

^{12}C cross sections

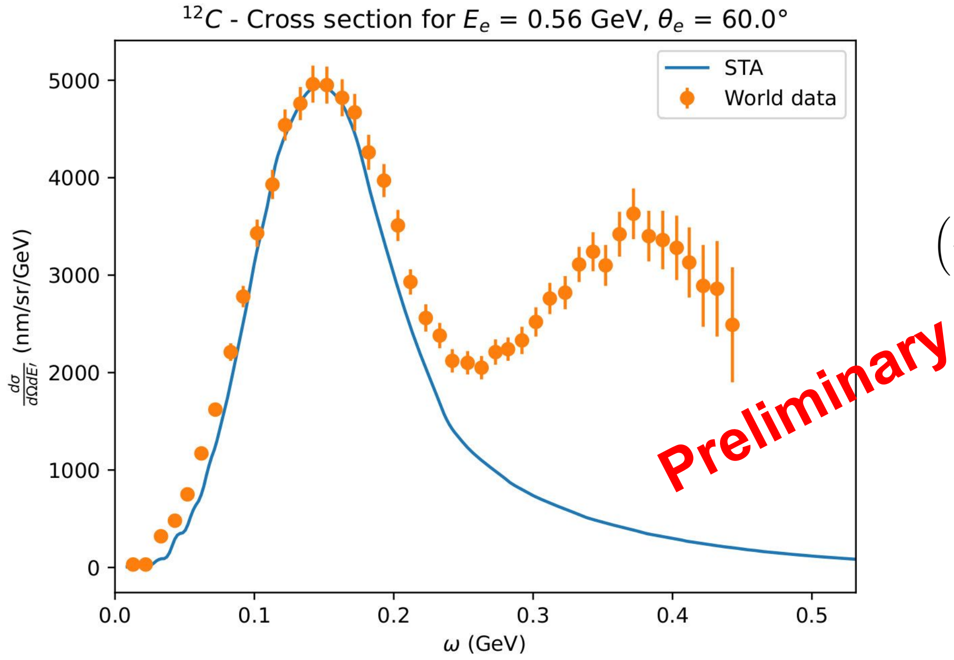

$$\left(\frac{d^2\sigma}{dE'd\Omega'}\right)_e = \left(\frac{d\sigma}{d\Omega'}\right)_{\mathrm{M}} \left[\left(\frac{q^2}{\mathbf{q}^2}\right)^2 R_L(|\mathbf{q}|,\omega) + \left(\tan^2\frac{\theta}{2} - \frac{1}{2}\frac{q^2}{\mathbf{q}^2}\right) R_T(|\mathbf{q}|,\omega)\right]$$

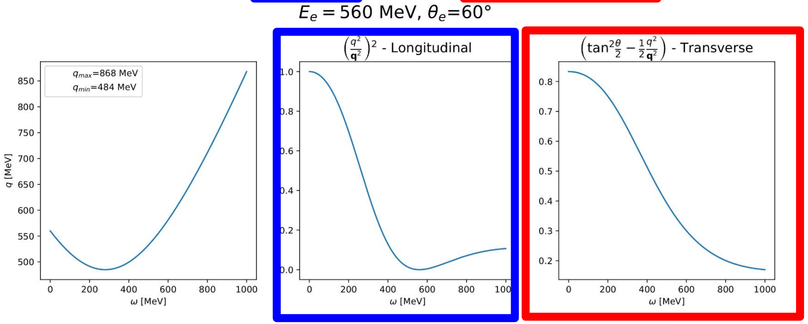

NC processes on deuteron with STA

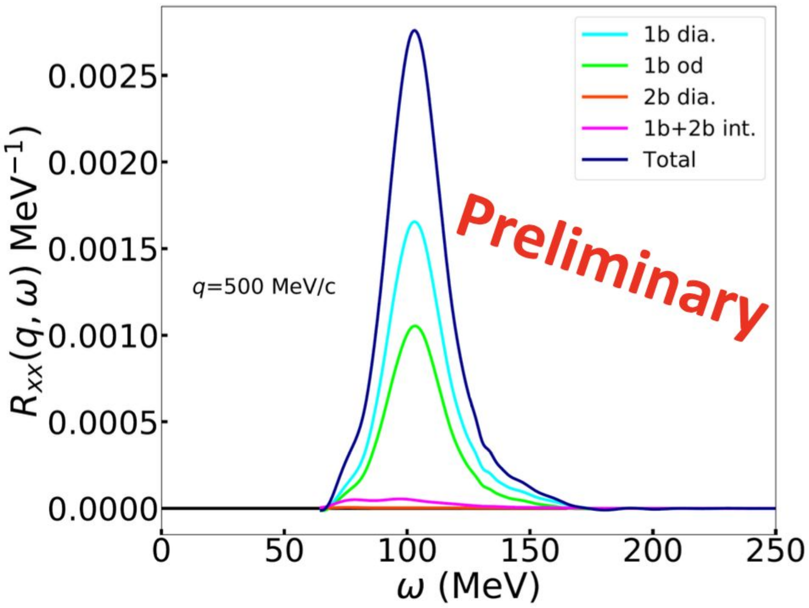

Garrett King *et al.* in preparation

Ties to fundamental symmetry: CKM unitarity

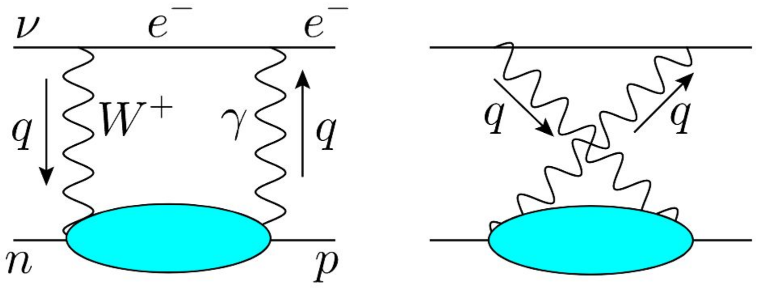

Superallowed beta decay used to test CKM unitarity

Radiative corrections receive contributions from the QE region

$$\frac{\log 2}{ft} = \frac{G_F^2 m_e^5 |V_{ud}|^2}{\pi^3}(1 + \Delta_R^V + \delta_R' + \delta_{NS} - \delta_C)$$

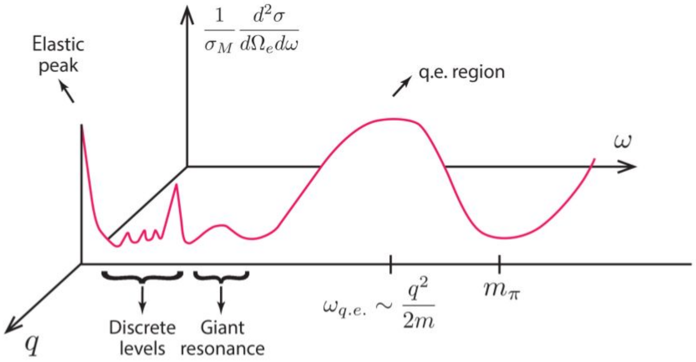

Momentum distributions

Nuclear properties are strongly affected by two-body correlations and currents in a wide range of energy and momentum transfer

Two-body momentum distribution
Wiringa *et al.* PRC89(2014)024305

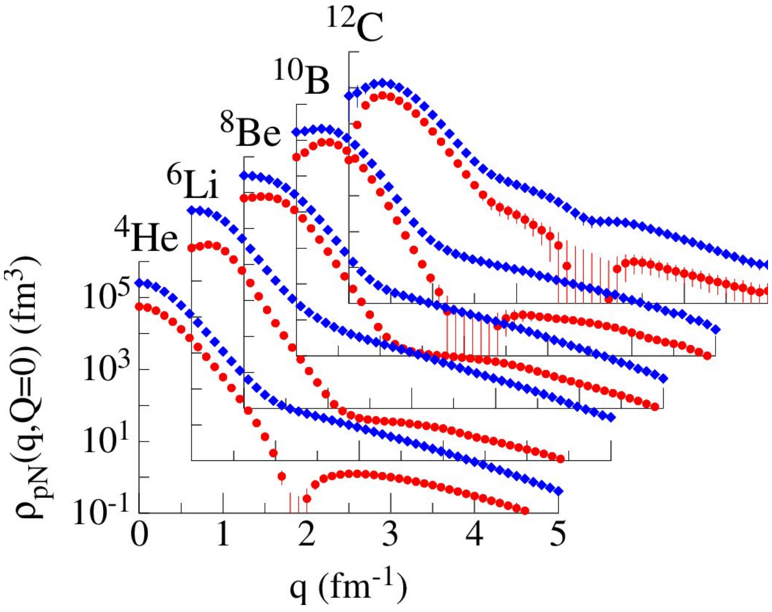

pp-pairs; np-pairs

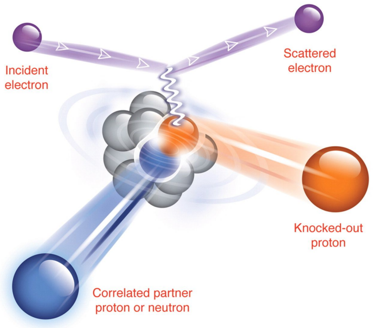

New two-body momentum distributions from chiEFT potentials

Piarulli, SP, Wiringa PRC (2023)

Two-body densities

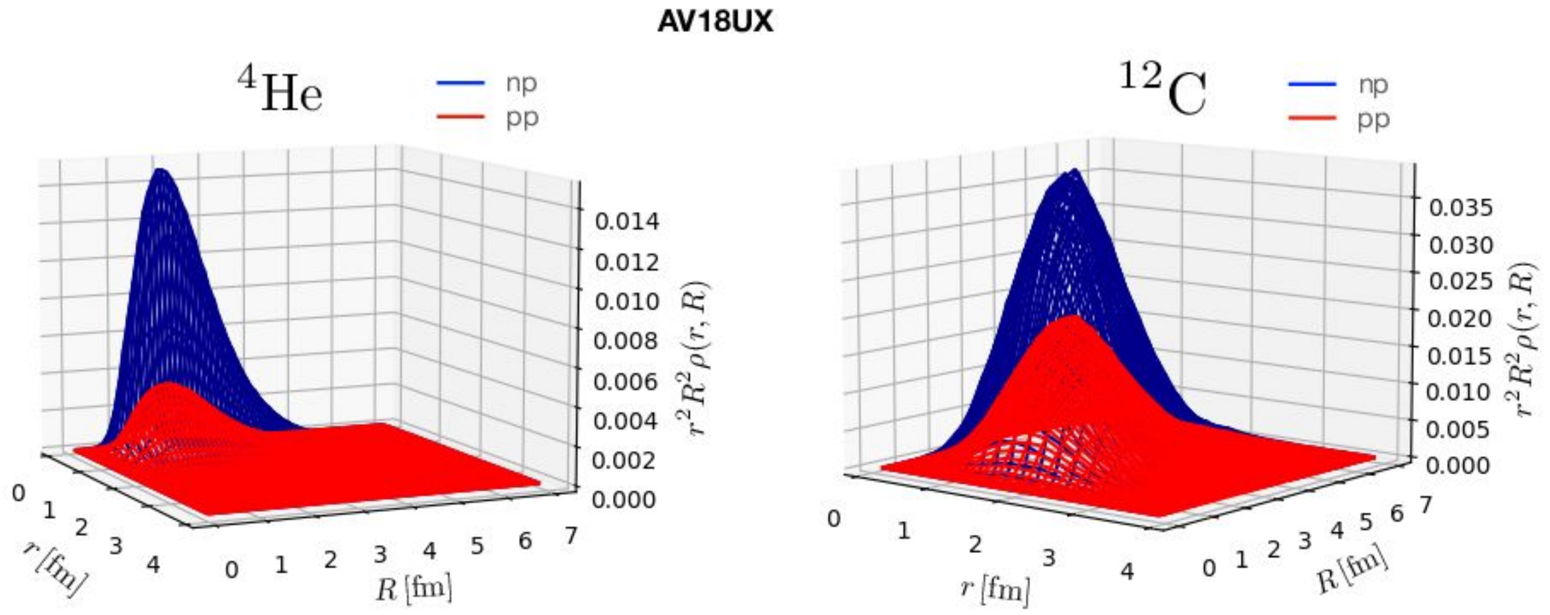

Piarulli, SP, Wiringa PRC (2023)

data

Summary

Ab initio calculations of light nuclei yield a picture of nuclear structure and dynamics where many-body effects play an essential role to explain available data.

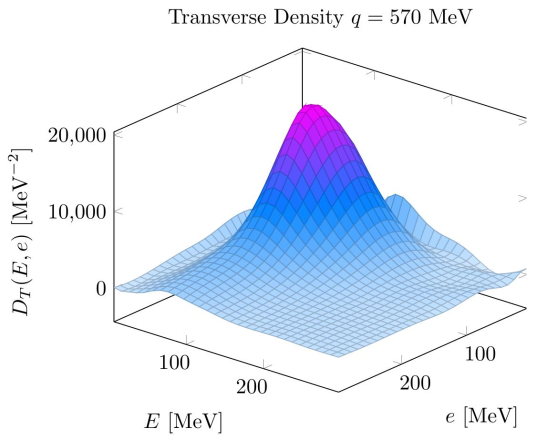

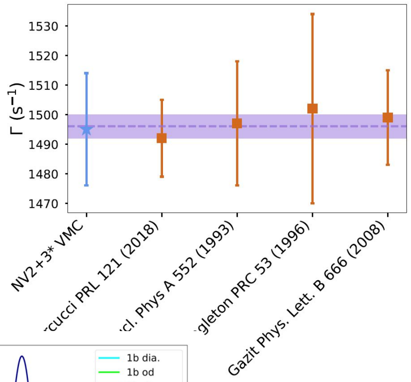

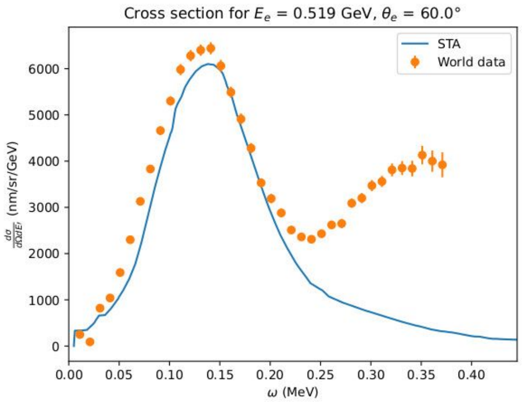

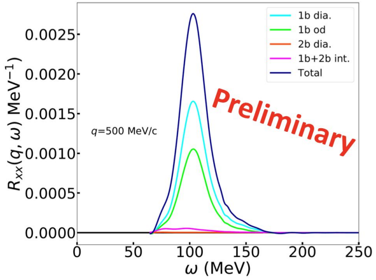

Close **collaborations** between NP, **LQCD**, **EFT**, **Pheno**, **Hep**, **Comp**, **Expt**, …
are required to progress
e.g., NP is represented in the Snowmass process and LRP

It's a very exciting time!

Nuclear Theory for New Physics NP&HEP TC

Nuclear Theory for New Physics

- About Us
- Commitment to Diversity
- Funding Acknowledgement

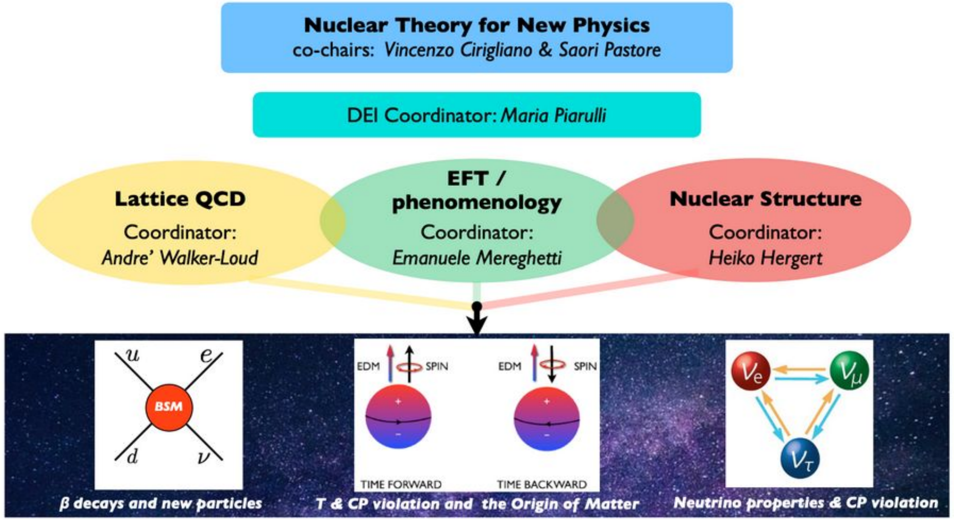

Funding Acknowledgement

We are funded in part through The Department of Energy, Office of Science, Office of Nuclear Physics and the Office of High Energy Physics

NTNP

Snowmass:
Topical groups and Frontier Reports, Whitepapers, …

LRP:
White papers, 2301.03975, FSNN, …

Collaborators

WashU: **Andreoli Bub Chambers-Walls King McCoy Piarulli**
LANL: Baroni Carlson Cirigliano Gandolfi Hayes Mereghetti
JLab+ODU: Schiavilla Gnech
ANL: Lovato Rocco Wiringa
UCSD/UW: Dekens
Pisa U/INFN: Kievsky Marcucci Viviani
Salento U: Girlanda
Huzhou U: Dong Wang
Fermilab: Gardiner Betancourt
MIT: Barrow

Washington University in St. Louis
Arts & Sciences

Theory Alliance
FACILITY FOR RARE ISOTOPE BEAMS

U.S. DEPARTMENT OF ENERGY INCITE LEADERSHIP COMPUTING

Los Alamos NATIONAL LABORATORY EST. 1943

Argonne NATIONAL LABORATORY

U.S. DEPARTMENT OF ENERGY | Office of Science

McDonnell Center for the Space Sciences

Fermilab

Washington University in St. Louis
Arts & Sciences

Department of Physics

McDonnell Center for the Space Sciences

Quantum Monte Carlo Group for Nuclear Physics

https://physics.wustl.edu/quantum-monte-carlo-group

Lorenzo Andreoli
Postdoctoral Research Associate

landreoli@wustl.edu

Jason Bub
Graduate Student

jason.bub@wustl.edu

Garrett King
Graduate Student

kingg@wustl.edu

Anna McCoy
FRIB Theory Fellow

&

Quantum Monte Carlo Methods

Minimize the expectation value of the nuclear Hamiltonian: H = T +v_{ij} + V_{ijk}

$$E_V = \frac{\langle \Psi_V | H | \Psi_V \rangle}{\langle \Psi_V | \Psi_V \rangle} \geq E_0$$

using the trial wave function:

$$|\Psi_V\rangle = \left[\mathcal{S}\prod_{i<j}(1 + U_{ij} + \sum_{k\neq i,j} U_{ijk})\right]\left[\prod_{i<j} f_c(r_{ij})\right]|\Phi_A(JMTT_3)\rangle$$

Further improve the trial wave function by eliminating spurious contaminations via a Green's Function Monte Carlo propagation in imaginary time

$$\Psi(\tau) = \exp[-(H - E_0)\tau]\Psi_V = \sum_n \exp[-(E_n - E_0)\tau]a_n\psi_n$$

$$\Psi(\tau \to \infty) = a_0\psi_0$$

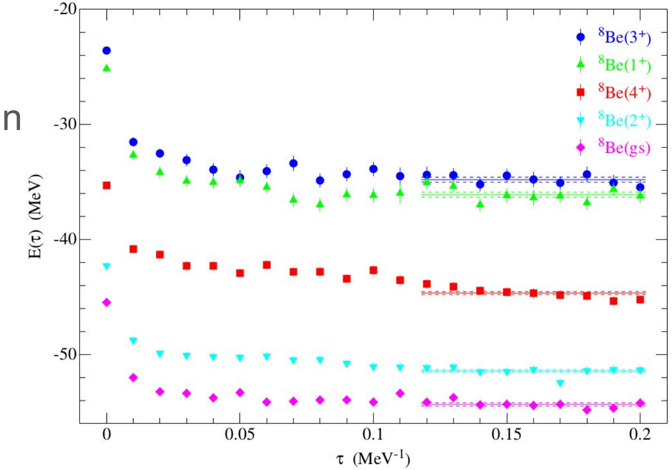

Carlson, Wiringa, Pieper *et al.*

Norfolk Two- and Three-body Potentials

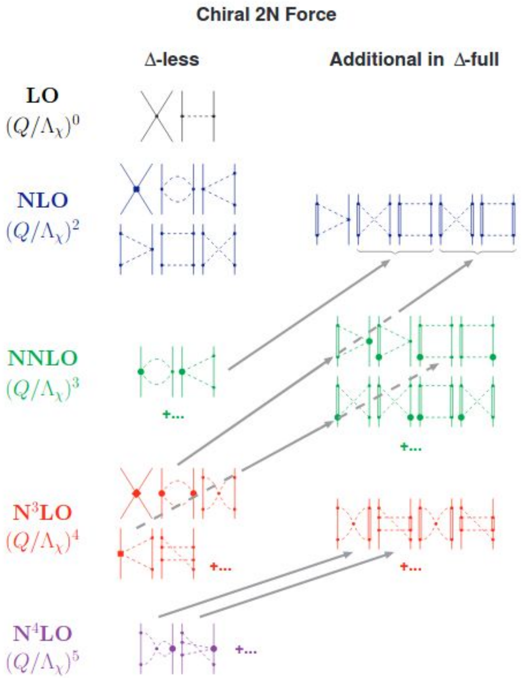

Norfolk Chiral Potentials

NV2+3

developed in Piarulli *et al*.
PRC91(2015)024003
PRC94(2016)054007

26 LECs fitted to np and pp Granada database (2700-3700 data points; 125-200 MeV) with a chi-square/datum ~1

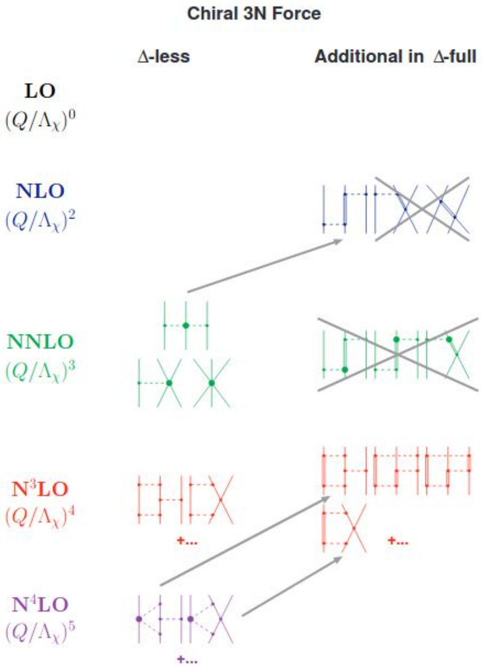

Figs. credit Entem and Machleidt Phys.Rept.503(2011)1

Optimization of Nuclear Two-body Interactions

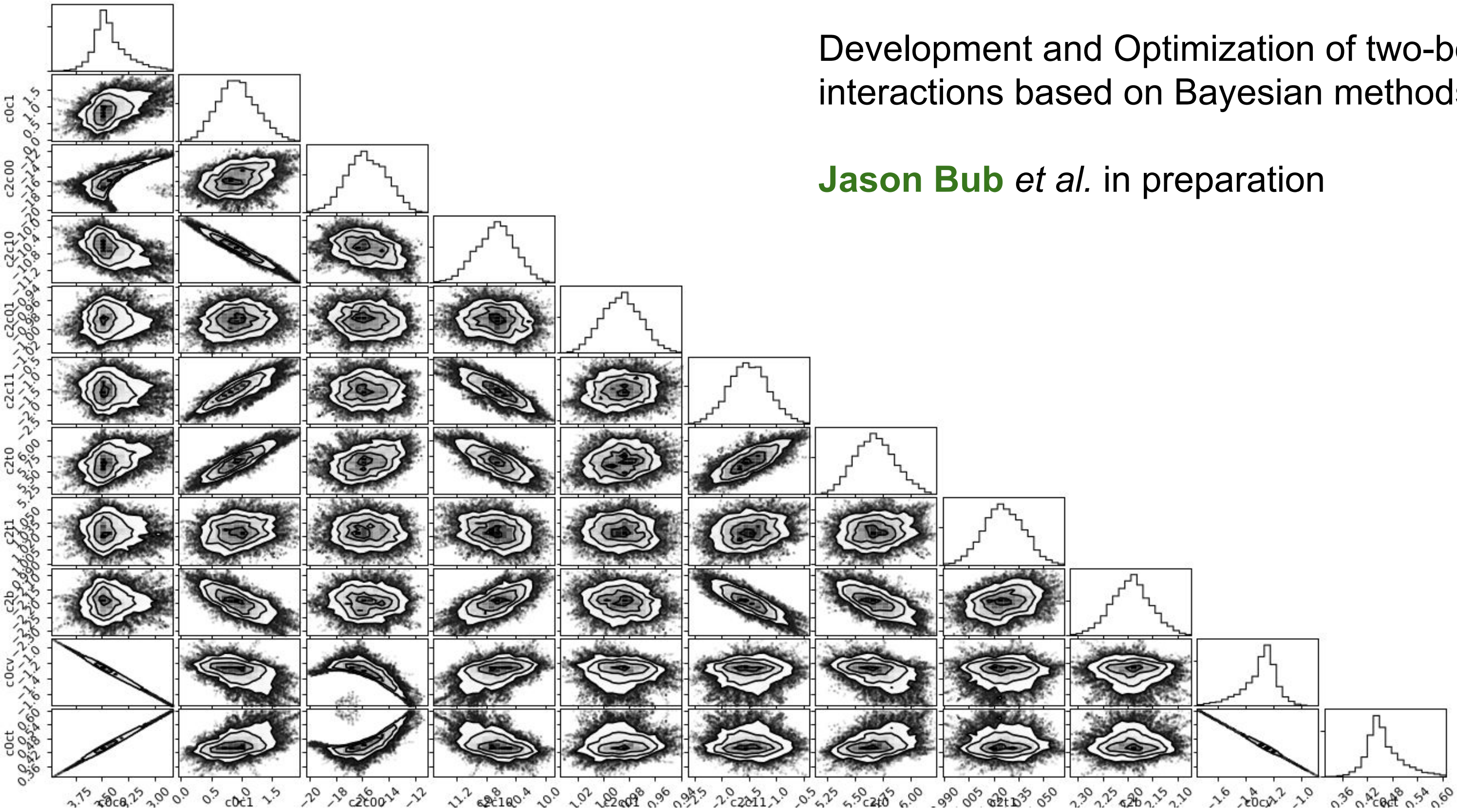

Development and Optimization of two-body interactions based on Bayesian methods

Jason Bub *et al.* in preparation

Three-body Force and the Axial Contact Current

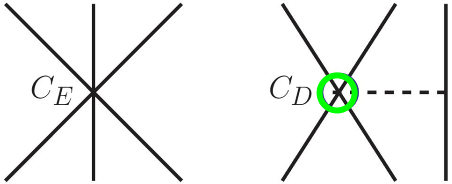

Three-body force

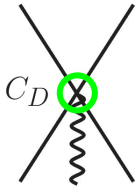

Axial two-body contact current

LECs c_D and c_E are fitted to:

- **trinucleon B.E.** and ***nd*** **doublet scattering length** in **NV2+3-Ia**
- **trinucleon B.E.** and **Gamow-Teller matrix element of tritium** **NV2+3-Ia***

Baroni *et al.* PRC98(2018)044003

Energies A=8-10 slightly better with non-starred models

Fitting strategies

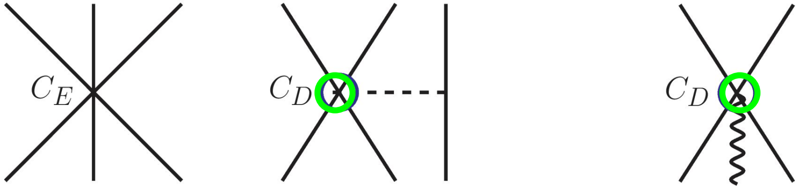

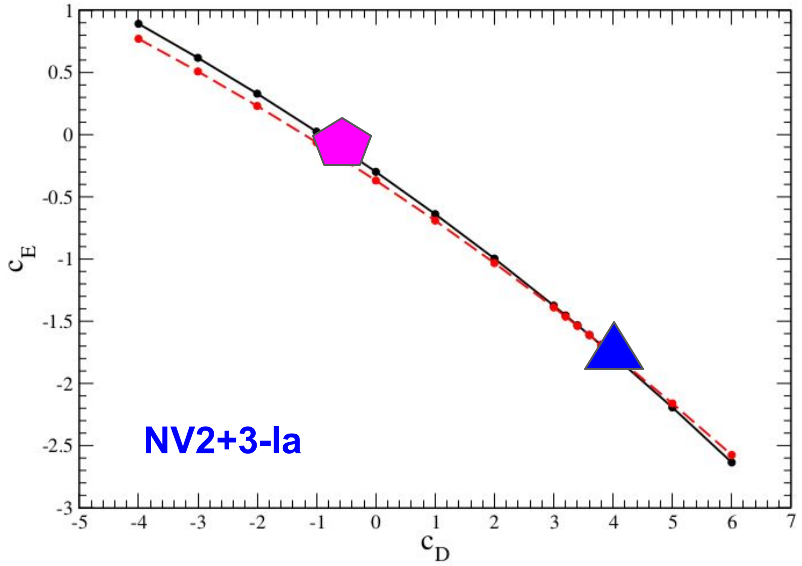

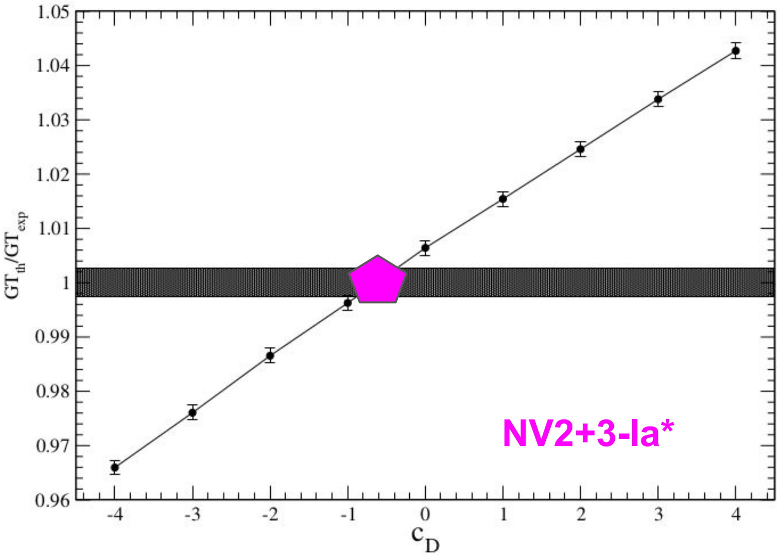

Baroni *et al.* PRC98(2018)044003

Contact Current

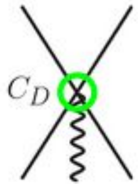

	NV2+3-Ia	NV2+3-Ia*
c_D	3.666	-0.635
c_E	-1.638	-0.090
z_0	0.090	1.035

$$\mathbf{j}_{5,a}^{\mathrm{N3LO}}(\mathbf{q};\mathrm{CT}) = z_0\, \mathrm{e}^{i\,\mathbf{q}\cdot\mathbf{R}_{ij}}\, \frac{\mathrm{e}^{-\tilde{r}_{ij}^2}}{\pi^{3/2}}\, (\boldsymbol{\tau}_i \times \boldsymbol{\tau}_j)_a\, (\boldsymbol{\sigma}_i \times \boldsymbol{\sigma}_j)$$

$$z_0 = \frac{g_A}{2}\,\frac{m_\pi^2}{f_\pi^2}\,\frac{1}{(m_\pi R_S)^3}\left[-\frac{m_\pi}{4 g_A \Lambda_\chi}\, c_D + \frac{m_\pi}{3}\,(c_3 + 2c_4) + \frac{m_\pi}{6m}\right]$$

Beta Decay and Electron Capture in Light Nuclei

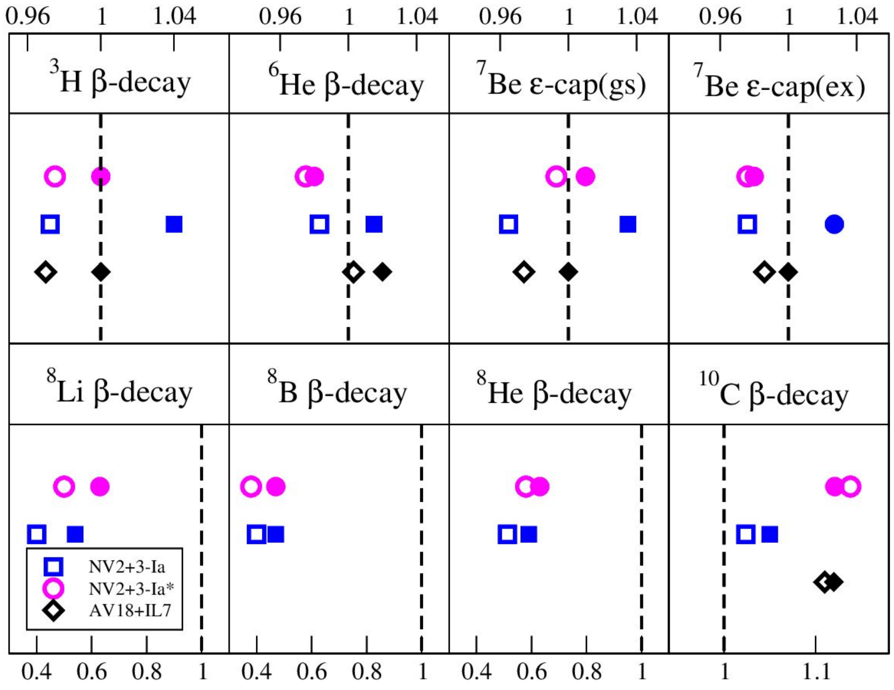

Garrett King *et al.* PRC102(2020)025501

Calculations based on

- chiral interactions and currents
  NV2+3-Ia Norfolk unstarred
  NV2+3-Ia* Norfolk* starred
  Piarulli *et al.* PRL120(2018)052503
  Baroni *et al.* PRC98(2018)044003
- phenomenological **AV18+IL7** potential and chiral axial currents (hybrid calculation)

Two-body currents are small/negligible;
Results for A=6-7 are within 2% of data;
Results for A=8 are off by a 30-40%;
Results for A=10 are affected by the second $J^{\pi}=(1^{+})$ state in ^{10}B

Axial Two-body Transition Density

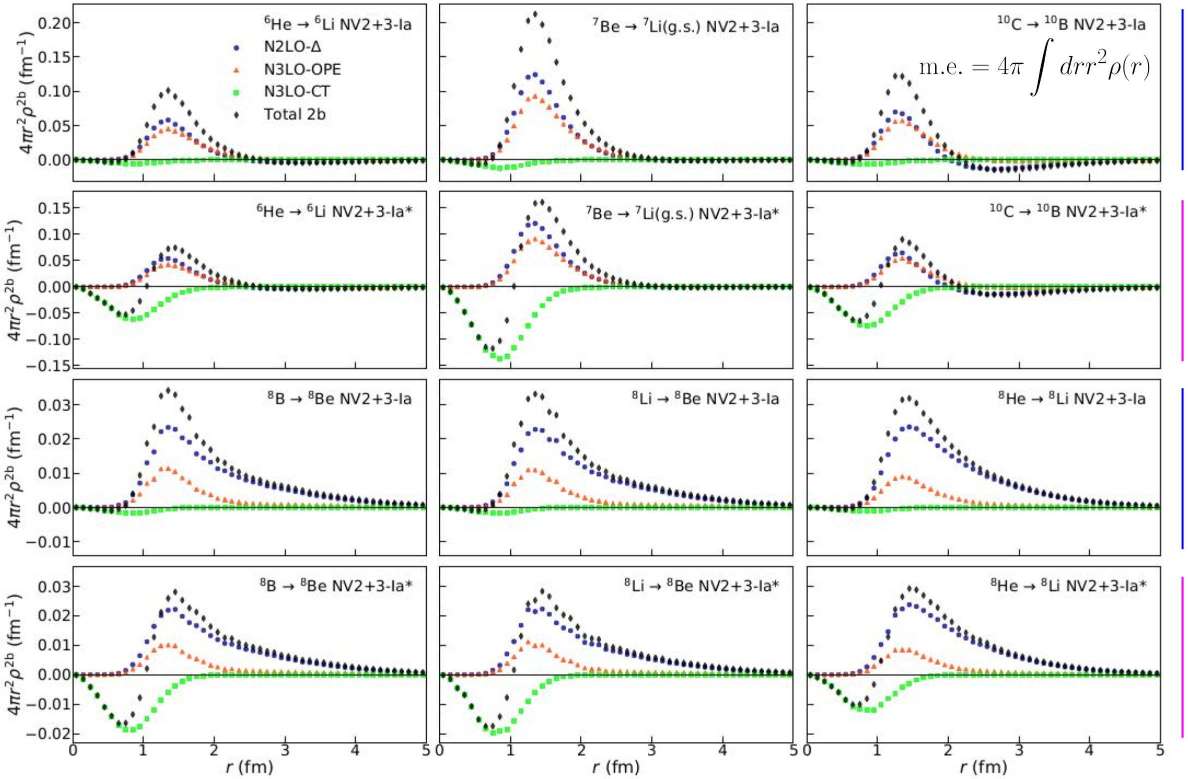

Garrett King *et al.* PRC102(2020)025501

NV2+3-Ia ; NV2+3-Ia*

enhanced contribution from contact current in the starred model gives rise to nodes in the two-body transition density

Two-body axial currents

long-range at N2LO and N3LO

contact current at N3LO

Scaling & Universality of Short-Range Dynamics

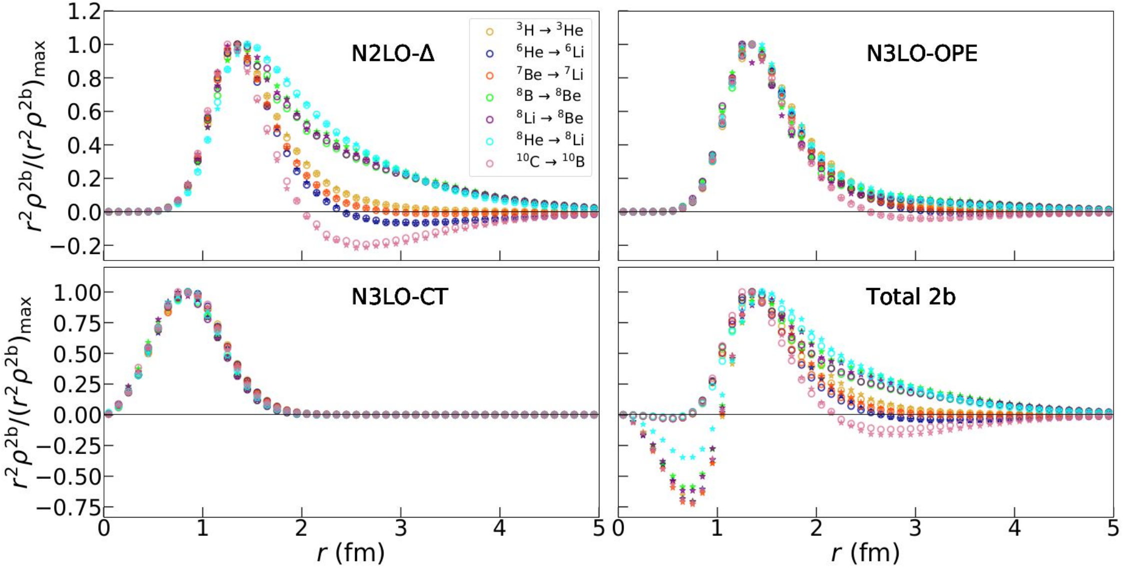

Garrett King *et al.* PRC102(2020)025501

NV2+3-Ia empty circles; NV2+3-Ia* stars
Different colors refer to different transitions

Dark Matter

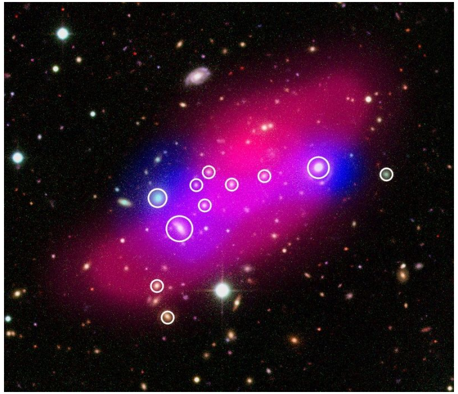

ESA, XMM-Newton, Gastaldello, CFHTL

Candidates

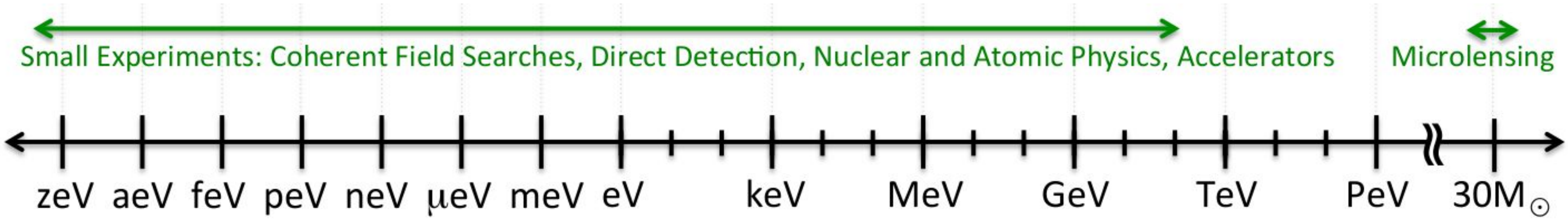

US cosmic vision 2017

Beta decay spectrum

^{6}He Beta decay spectrum for BSM searches with NCSL, He6-CRES, LPC-Caen

^{6}He beta-decay spectrum from NCSM

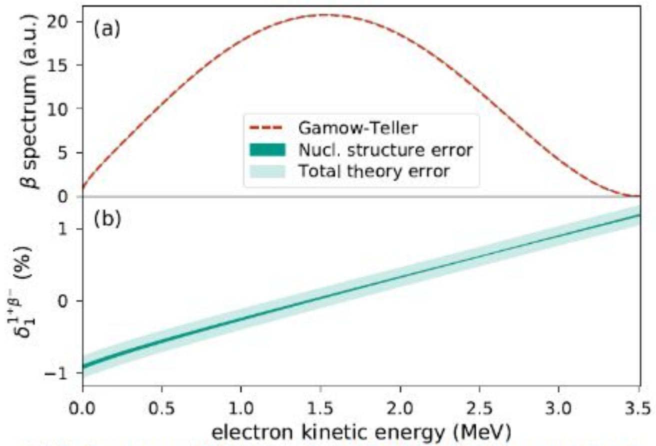

Glick-Magid et al. arXiv:2107.10212

$$\frac{d\Gamma}{d\varepsilon} = \frac{d\Gamma_0}{d\varepsilon} \times (1 + \text{corrections})$$

^{6}He Beta Decay Spectrum

$$d\Gamma = \frac{2\pi}{2J_i+1} \sum_{s_e, s_\nu} \sum_{M_i, M_f} |\langle f | H_W | i \rangle|^2 \delta(\Delta E) \frac{d^3 k_e}{(2\pi)^3} \frac{d^3 k_\nu}{(2\pi)^3}$$

Multipoles

$$\begin{aligned}
C_1(q;A) &= \frac{i}{\sqrt{4\pi}} \langle {}^6\mathrm{Li}, 10 | \rho_+^\dagger(q\hat{\mathbf{z}};A) | {}^6\mathrm{He}, 00 \rangle \\
L_1(q;A) &= \frac{i}{\sqrt{4\pi}} \langle {}^6\mathrm{Li}, 10 | \hat{\mathbf{z}} \cdot \mathbf{j}_+^\dagger(q\hat{\mathbf{z}};A) | {}^6\mathrm{He}, 00 \rangle \\
E_1(q;A) &= -\frac{i}{\sqrt{2\pi}} \langle {}^6\mathrm{Li}, 10 | \hat{\mathbf{z}} \cdot \mathbf{j}_+^\dagger(q\hat{\mathbf{x}};A) | {}^6\mathrm{He}, 00 \rangle \\
M_1(q;V) &= -\frac{1}{\sqrt{2\pi}} \langle {}^6\mathrm{Li}, 10 | \hat{\mathbf{y}} \cdot \mathbf{j}_+^\dagger(q\hat{\mathbf{x}};V) | {}^6\mathrm{He}, 00 \rangle
\end{aligned}$$

$$\begin{aligned}
C_1(q;A) &= -i\frac{qr_\pi}{3}\left(C_1^{(1)}(A) - \frac{(qr_\pi)^2}{10}C_1^{(3)}(A) + \mathcal{O}\left((qr_\pi)^4\right)\right) \\
L_1(q;A) &= -\frac{i}{3}\left(L_1^{(0)}(A) - \frac{(qr_\pi)^2}{10}L_1^{(2)}(A) + \mathcal{O}\left((qr_\pi)^4\right)\right) \\
M_1(q;V) &= -i\frac{qr_\pi}{3}\left(M_1^{(1)}(V) - \frac{(qr_\pi)^2}{10}M_1^{(3)}(V) + \mathcal{O}\left((qr_\pi)^4\right)\right) \\
E_1(q;A) &= -\frac{i}{3}\left(E_1^{(0)}(A) - \frac{(qr_\pi)^2}{10}E_1^{(2)}(A) + \mathcal{O}\left((qr_\pi)^4\right)\right)
\end{aligned}$$

Beta Decay Spectrum

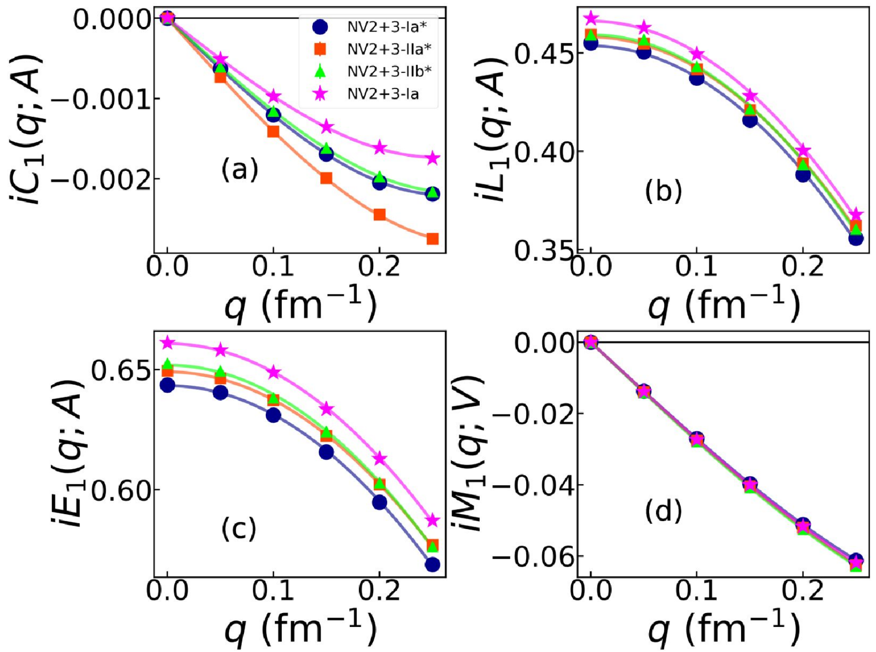

Dominant terms $L_1^{(0)}$ and $E_1^{(0)}$ have model dependence of ~1% to ~2%

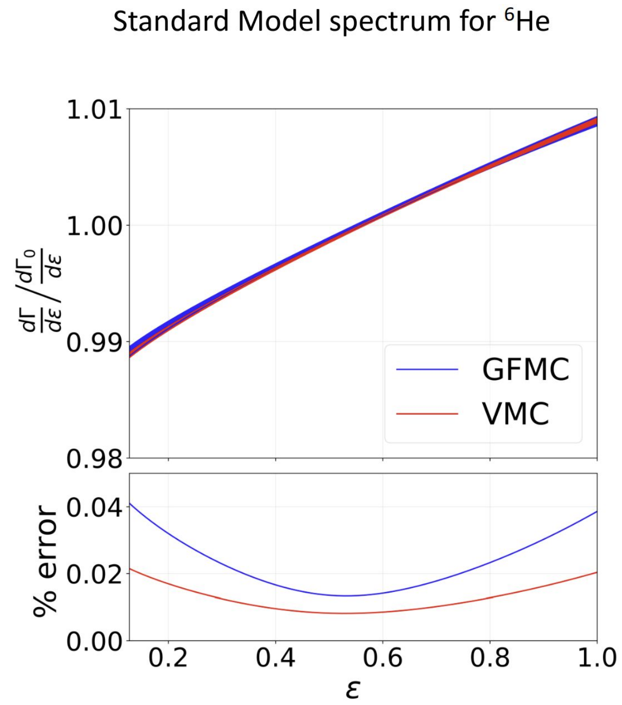

$\varepsilon = \frac{E_e}{\omega}$

τ_{GFMC} = 808 +/- 24 ms

$\tau_{Expt.}$ = 807.25 +/- 0.16 +/- 0.11 ms

Garrett King et al. PRC (2023)